AD-A034 034 AIR FORCE INST OF TECH WRIGHT-PATTERSON AFB OHIO SCH--ETC F/G 20/4
GAS BREAKDOWN CALCULATION: A COMPARATIVE STUDY.(U)
DEC 76 D A KLOC

UNCLASSIFIED GEP/PH/76-7 NL

1 OF 1
AD A034 034

END

DATE FILMED
2-77

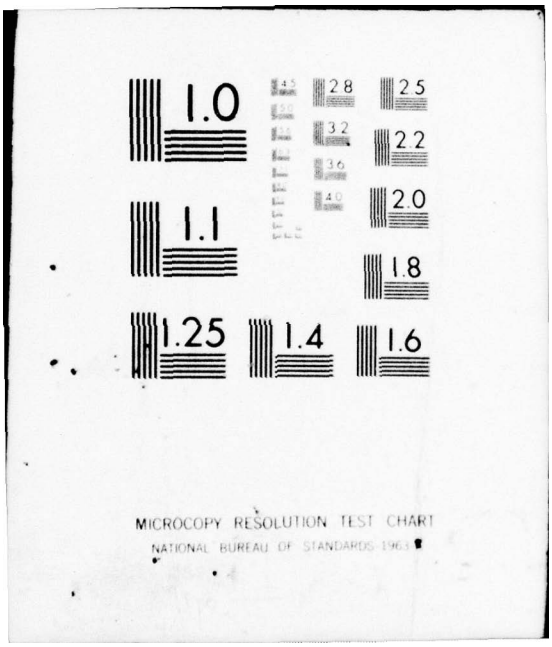
1.0
1.1
1.25
1.4
1.6
2.0
1.8
2.2
2.5
2.8
3.2
3.6
4.0
MICROCOPY RESOLUTION TEST CHART
NATIONAL BUREAU OF STANDARDS-1963

ADA034034

UNITED STATES AIR FORCE

AIR UNIVERSITY

AIR FORCE INSTITUTE OF TECHNOLOGY

Wright-Patterson Air Force Base, Ohio

Copy available to DDC does not permit fully legible reproduction

DDC
JAN 4 1977
B

GEP/PH/76-7

(9) Master's thesis,

(6) GAS BREAKDOWN CALCULATION:
A COMPARATIVE STUDY.

THESIS

(14) GEP/PH/76-7

(10) David A. Kloc
Capt USAF

(11) Dec 76

(12) 93p.

ACCESSION for
NTIS White Section
DDC Buff Section
UNANNOUNCED
JUSTIFICATION
BY
DISTRIBUTION/AVAILABILITY CODES
Dist. AVAIL. and/or SPECIAL
A

Approved for public release; distribution unlimited

012 225 dn

GEP/PH/76-7

GAS BREAKDOWN CALCULATIONS:
A COMPARATIVE STUDY

THESIS

Presented to the Faculty of the School of Engineering
of the Air Force Institute of Technology
Air University
in Partial Fulfillment of the
Requirements for the Degree of
Master of Science

by
David A. Kloc, B.S.
Capt USAF
Graduate Engineering Physics
December 1976

Approved for public release; distribution unlimited

Preface

Although the phenomenon of laser induced gas breakdown has been extensively studied for several years, little progress has been made in developing a simple model which can quickly and accurately predict breakdown at low values of incident flux. The investigations described in this thesis represent an attempt to develop such a model. While success was limited, it is hoped that the information presented here might prove to be a valuable starting point for anyone desiring to continue investigation of this problem.

I would like to extend my sincere appreciation to my advisor, Capt. P. E. Nielsen, who suggested this problem and provided the guidance needed to successfully complete this project. I would also like to thank Mrs. Mildred C. Kelley for her aid in the proofreading and preparation of the final report.

Finally, my deepest appreciation is extended to my wife, Mary, who was a source of encouragement and inspiration not only during this project, but throughout my eighteen months of study at AFIT.

Contents

	Page
Preface	ii
List of Figures	v
List of Tables	vi
Abstract	vii
I. Introduction	1
II. Backround	4
Breakdown(A Qualitative Discussion)	4
The Boltzmann Equation	8
A Temperature Model	10
The Quantum Kinetic Equation	14
A Diffusion Model	16
III. Approach	19
The Model Atom	19
Cross Sections and Rates	19
The Quantum Kinetic Model	23
The Temperature Model	25
Solution and Comparison	27
An Improved Diffusion Model	28
A Two-Temperature Model	31
IV. Analysis and Discussion	35
The Temperature Model	35
The Improved Diffusion Model	54
The Two-Temperature Model	55
V. Conclusion	58
Bibliography	60
Appendix A: Cross Sections	62
Appendix B: Rates	64
Appendix C: Derivation of the Temperature Model	67
Appendix D: Numerical Solution of the Quantum Kinetic Model	70
Appendix E: Numerical Solution of the Temperature Model	74

Contents

		Page
Appendix F:	Derivation of the Second Energy Moment of the Boltzmann Equation	77
Appendix G:	Numerical Solution of the Two-Temperature Model	79

List of Figures

Figure		Page
1	Cross Section for Ionization	21
2	Electron Growth Rate	36
3	Electron Distribution at 5×10^8 W/cm^2	38
4	Electron Distribution at 10^{11} W/cm^2	45

List of Tables

Table		Page
I	Apportionment of Energy Losses	40
II	Average Electron Energy	41
III	Cascade Growth Rates for Two and Three Level Atoms	43
IV	Cascade Growth Rates at Various R_{12}^{x}	46
V	Cascade Growth Rates at Various R_{1}^{I}	48
VI	Cascade Growth Rates at Various Values of Ground State Energy	50
VII	Cascade Growth Rates at Various Values of First Excited State Energy	52
VIII	Diffusion Model Growth Rates	54
IX	Two-Temperature Model Growth Rates	56
X	Rates for Ionization and Excitation	66

Abstract

An attempt is made to develop a simple yet accurate gas breakdown model which can be easily coupled to the hydrodynamic equations governing fluid flow in laser-target interactions. The accuracy of three relatively simple models is investigated. Each is compared with the more accurate and complex quantum kinetic model, to determine the conditions under which it maintains reasonable accuracy. A gas consisting of a single monatomic species is assumed and attention is restricted to the early portion of the electron cascade. A temperature model is found to agree reasonably well with the quantum kinetic model at values of incident laser flux greater than 5×10^9 W/cm^2. A diffusion model is found to yield similar results. A two-temperature model, which is derived in an attempt to extend the range of the temperature model to lower values of incident flux, is found to be invalid.

I. Introduction

The breakdown threshold of the atmosphere imposes an upper limit on the amount of energy which can be propagated through the atmosphere by a laser. Below this rather well pronounced threshold intensity, the atmosphere is relatively transparent to the laser beam. However, once the threshold is exceeded cascade ionization ensues. Naturally occurring electrons are rapidly heated by the laser radiation. Those attaining sufficient energy ionize neutral species and create more electrons. The net result is the formation of a highly ionized plasma which severely attenuates the beam. Similarly, vapor emerging from a target irradiated by a laser can break down and shield the target from further deposition of laser radiation.

Under the sustained action of a laser, several interesting post-breakdown effects will emerge. The newly formed plasma continues to absorb almost all the energy incident on it, heating the gas in the absorption region to very high temperatures. As this relatively small volume of gas begins to expand, the surrounding air is heated and becomes ionized. This causes a new layer of gas capable of absorbing energy to be formed within the beam's column, and a "laser absorption wave" will propagate towards the laser,decoupling it from the target. At very high laser intensities, the hot gases will expand so rapidly that a shock wave, capable of interacting with the

target,will be formed.

If these hydrodynamic phenomena associated with laser-target interaction are to be properly analyzed, an accurate prediction of the breakdown threshold is required. Present calculations of breakdown phenomena(the quantum kinetic model) use lengthy computer programs which, even when simplified, require an average of 30 seconds for each run. These calculations must be repeated at least 300 times for each centimeter the shock wave travels. Consequently, there exists a need for a simple yet accurate breakdown model which could be easily coupled to the equations governing fluid flow in a laser-target interaction.

In an effort to find such a model, three relatively simple breakdown models were investigated. The accuracy of each was determined through a comparison with the more accurate quantum kinetic model. Primary emphasis was placed on comparisons involving a temperature model. This model assumes a maxwellian distribution of free electrons. The second model compared, a diffusion model, assumes that electron heating can be represented as a diffusion of free electrons along the energy axis. Finally, a two-temperature model which assumes a segmented electron distribution function was developed and its results compared to those of the quantum kinetic model.

A brief review of the theory involved in laser induced gas breakdown is presented in Chapter II. Chapter III provides a discription of both the comparisons made and

the models compared. Results are presented and discussed in Chapter IV followed by conclusions and recommendations in Chapter V.

II. Backround

Although the breakdown of gases has been studied extensively for many years, gas breakdown under the action of radiation at optical frequencies is a more recently observed(1962) phenomenon. Since fluxes intense enough to produce breakdown at optical frequencies can only be produced by a laser, it is within this context that the phenomenon is studied. The theory involved has been firmly established and will be discussed in this chapter. The first part of this chapter is devoted to a qualitative discussion of the processes involved, while the remainder of the chapter will deal with some of the major theories utilized to explain breakdown.

Breakdown (A Qualitative Discussion)

The breakdown of a gas will occur if, during the time of the laser pulse, the gas can absorb enough energy to achieve and maintain a high degree of ionization. Processes which could account for this ionization are the absorption of photons by a neutral atom, inelastic collisions between atoms and electrons, and a combination of both processes. Those processes which could reduce the degree of ionization are the recombination of electrons and ions, and the diffusion of the charged particles from the volume of the gas upon which the laser radiation is incident.

The direct ionization of atoms by laser photons was studied extensively by Keldysh(Ref 1). Since, in most cases, the value of the ionization energy(5-20 eV) is much greater than the photon energy(0.1-1.5 eV) it is impossible for one photon to ionize the atom. However, if $I/\hbar\omega$ photons can be absorbed simultaneously by an atomic electron, ionization would be possible. At atmospheric pressure the laser intensities required to produce breakdown by this mechanism are much greater than those under which breakdown is observed experimentally. Thus, the "multiquantum photoeffect" is not considered to be a likely breakdown mechanism.

The process of electron cascade ionization(Ref 2) has been accepted as the mechanism most likely involved in breakdown. The cascade can begin with a single "priming electron". This electron absorbs light quanta during collisions with atoms. Along with this inverse bremsstrahlung absorption of energy by the electrons there occurs a stimulated bremsstrahlung emission. The absorption, however, is more likely than emission so that over a period of time a net absorption of energy occurs. This net absorption of energy can be thought of as a diffusion of the electron along a one-dimensional energy axis. If excitational processes are temporarily ignored, the energy of the electron will continue to increase until it exceeds the ionization potential of the neutral atoms. It will then collide inelastically with one of the atoms and ionize it.

The result will be two electrons of very low energy replacing the one electron with energy slightly greater than I. These two electrons can now absorb energy and repeat the process. This cascade will continue until breakdown is achieved.

Energetic electrons, however, are also capable of causing excitations. Since excitation requires less energy than ionization an electron may lose its energy to excitation many times before acquiring an energy sufficient for an ionization. Under conditions of sufficiently high flux, atoms excited into higher atomic states can be rapidly ionized by the absorption of two or three quanta. In this case an excitation is equivalent to an ionization and the cascade continues unhindered. At lower fluxes and photon energies of less than about 1 eV, photoionization of the excited states becomes unlikely(for the same reason as multiphoton ionization) and energy going into excitations slows the development of the cascade. Once an atom is excited the probability that it will encounter a second electron and be ionized is extremely small except during the latter stages of the cascade when the density of electrons and excited atoms is high(Ref 3:658).

The development of the cascade can also be hindered by diffusion of the free electrons from the region of action of the incident radiation. The diffusion losses will be smaller at higher pressures and larger beam diameters. At fluxes of interest($S > 10^7 W/cm^2$), diffusion losses can

be assumed to be negligible at pressures greater than 1 atm and beam diameters larger than 10^{-2}cm(Ref 2:773). Another mechanism that will hinder the cascade is three body recombinations. This mechanism, however, is not considered significant since losses due to it will only be observed very late in the cascade.

Since at least one electron must be present for the cascade to proceed, the question of the origin of the first electron is often raised. The presence of a small quantity of easily ionizable impurity atoms is one source. The production of the first electron can then occur as a result of photoionization or collision involving the impurity atom. Another source of electrons is the atmosphere. Non-equilibrium atmospheric effects such as cosmic radiation result in an average free electron density of $100/cm^2$. Therefore, under appropriate conditions, the first electron can be found.

Finally, if R is defined to be the cascade growth rate then the number of free electrons at any time t can be expressed by

$$n_e = n_e^o \, e^{Rt} \tag{1}$$

where n_e^o is the initial free electron density. Now, if the breakdown criterion is chosen to be the achievement of a specific electron population n_e^1, then the time required for breakdown to occur is given by

$$t_1 = \tau \ln(n_e^1/n_e^o) \qquad (2)$$

where $\tau = 1/R$ is the cascade time constant. As can be seen from Eq (2) the occurrence of breakdown is not strongly dependent on the initial electron density. It is, however, highly dependent on the time constant τ which is in turn a strong function of the laser flux. It is for this reason that an abrupt breakdown threshold is found to exist(Ref 3:657).

The Boltzmann Equation

Early investigations revealed that the problem of laser induced gas breakdown could be best approached through the use of the Boltzmann equation

$$\frac{\partial f}{\partial t} + \bar{v}\cdot\nabla f + \bar{a}\cdot\nabla_v f = \left.\frac{\partial f}{\partial t}\right|_{coll} \qquad (3)$$

where f is the electron distribution function, $\bar{v}$ the electron velocity, $\bar{a}$ the electron acceleration, and $\left.\frac{\partial f}{\partial t}\right|_{coll}$ represents the change in f due to collisional processes. Under the assumption of spatial homogeneity of f the second term in Eq (3) vanishes.

In a manner identical to that used for microwave breakdown(Ref 4), an electron heating term can be derived. This term describes the rate at which an electron, acted upon by a field, gains energy on collision with an atom.

Under these conditions Newton's equation of motion for the electrons can be written as(Ref 4:170)

$$m_e \frac{d\bar{v}}{dt} + m_e \bar{v} \nu = e\bar{E}\, e^{-i\omega t} \tag{4}$$

where ν is the electron-atom collision frequency, e the electronic charge, and ω is the angular frequency of the applied field, $\bar{E}$. Solving Eq (4) for $\bar{v}$ yields

$$\bar{v} = \frac{eEe^{-i\omega t}}{m_e(\nu - i\omega)} \tag{5}$$

The third term of Eq (3) can be rewritten as

$$\bar{a}\cdot\nabla_v f = \bar{a}\ (m_e\bar{v})\ \frac{\partial f}{\partial \epsilon} \tag{6}$$

so that with $\bar{a} = \frac{e\bar{E}}{m_e} e^{-i\omega t}$ and $\bar{v}$ given by Eq (5), Eq (6) averaged over a period becomes

$$\bar{a}\cdot\nabla_v f = \frac{e^2E^2\nu}{m_e(\nu^2+\omega^2)}\ \frac{\partial f}{\partial \epsilon} \tag{7}$$

This equation can also be derived in a more rigorous manner directly from the Boltzmann equation(Ref 4:46-47,166). Substituting Eq (7) into Eq (3) yields a final form for the Boltzmann equation

$$\frac{\partial f(\epsilon)}{\partial t} + \frac{\dot{\epsilon}}{n_e}\frac{\partial f(\epsilon)}{\partial \epsilon} = \left.\frac{\partial f}{\partial t}\right|_{coll} \tag{8}$$

where f is defined to be a function of energy and $\dot{\epsilon}$ is given by

$$\dot{\epsilon} = \frac{n_e e^2 S \nu}{m_e c \epsilon_o (\nu^2+\omega^2)} \tag{9}$$

where the substitution $S = (\epsilon_o/2)E^2c$ was made in Eq (7), S being the laser flux in W/cm^2. Included in the collision term on the right side of Eq (8) are the rates of excitation and ionization as well as the rates of any other significant collisional processes.

A Temperature Model

If the collisional terms are written out explicitly Eq (8) becomes

$$\frac{\partial f(\epsilon)}{\partial t} + \frac{\dot{\epsilon}}{n_e}\frac{\partial f(\epsilon)}{\partial \epsilon} =$$

$$- \sum_{i,j>i} n_i R^x_{ij}(\epsilon) f(\epsilon) + \sum_{i,j>i} n_i R^x_{ij}(\epsilon + x_{ij}) f(\epsilon + x_{ij})$$

$$- \sum_j n_j R^I_j(\epsilon) f(\epsilon) + \sum_j n_j R^I_j(\epsilon + I_j) f(\epsilon + I_j)$$

$$+ \delta(\epsilon) \sum_j n_j \int_0^\infty R^I_j(\epsilon) f(\epsilon) d\epsilon + \bar{R} \tag{10}$$

where R^x_{ij} and R^I_j are the rates for excitation and ionization, x_{ij} and I_j represent the excitation and ionization energies, and the n_i are the population densities of the various atomic levels. The first four terms on the right

side of Eq (10) represent the rate at which electrons of energy ϵ are either gained or lost to the distribution as a result of excitation and ionization of atoms. The fifth term represents the rate at which electrons of zero energy are created by ionization. The last term, $\bar{R}$, represents all reverse rates(deexcitations, recombinations) and is assumed to be small during the early stages of breakdown if most of the atoms are originally assumed to be in a ground state.

Now, if the gas is assumed to be made up of atoms which possess a nucleus and two electronic levels, a ground state and an excited state, Eq (10) simplifies to

$$\frac{\partial f(\epsilon)}{\partial t} + \frac{\dot{\epsilon}}{n_e}\frac{\partial f(\epsilon)}{\partial \epsilon} =$$

$$-n_1 R^X(\epsilon) f(\epsilon) + n_1 R^X(\epsilon + x) f(\epsilon + x)$$

$$-n_1 R^I(\epsilon) f(\epsilon) + n_1 R^I(\epsilon + I) f(\epsilon + I)$$

$$+ \delta(\epsilon) \int_0^\infty n_1 R^I(\epsilon)\, f(\epsilon)\, d\epsilon \qquad (11)$$

At this point, the exact form of the electron distribution function is unknown. If it is assumed to be maxwellian,

$$f(\epsilon) = \frac{2}{} \frac{\epsilon^{1/2}}{T^{3/2}} e^{-\epsilon/T} \qquad (12)$$

where T is the electron temperature, then a temperature

model approach towards breakdown will emerge. Taking the zeroth energy moment of Eq (11) yields an equation for electron growth(Appendix C)

$$\frac{dn_e}{dt} = \langle R^I \rangle n_e n_1 \tag{13}$$

where $\langle R^I \rangle$, the ionization rate, is a function of temperature, obtained by averaging R^I over all energy. Taking the first energy moment yields an energy balance equation (Appendix C)

$$\frac{d\langle \epsilon \rangle}{dt} = \frac{\dot{\epsilon}}{n_e} - x\langle R^x \rangle n_1 - I\langle R^I \rangle n_1 - \frac{\langle \epsilon \rangle}{n_e}\frac{dn_e}{dt} \tag{14}$$

where $\langle \epsilon \rangle$, the average energy in eV, is given by $\frac{3}{2}$ T. Eqs (13)-(14) taken together can be used to investigate and predict many of the phenomena involved in breakdown and are often referred to as a "temperature model".

The conditions required for breakdown can now be estimated using Eqs (13)-(14). Under the assumption that the average electron energy equilibrates rapidly($t_{eq} \sim .1\tau$) Eq (14) becomes

$$\frac{\dot{\epsilon}}{n_e} = x\langle R^x \rangle n_1 + I\langle R^I \rangle n_1 + \langle \epsilon \rangle \langle R^I \rangle n_1 \tag{15}$$

where Eq (13) was also used. The rates can be expressed

as(Ref 5:388-390)

$$\langle R^x \rangle = R_o^x \, e^{-x/T} \tag{16}$$

and

$$\langle R^I \rangle = R_o^I \, e^{-I/T} \tag{17}$$

where R_o^x and R_o^I are slowly varying functions of T which can be assumed constant. For $R_o^x \approx R_o^I$ the last two terms on the right side of Eq (15) can be ignored. Solving Eq (15) for $e^{-x/T}$ yields

$$e^{-x/T} = \frac{\dot{\varepsilon}}{n_e n_1 x \, R_o^x} \tag{18}$$

Now, if both sides of Eq (18) are raised to the I/x power and the results substituted into Eq (17), $\langle R^I \rangle$ becomes

$$\langle R^I \rangle = R_o^I \left[\frac{\dot{\varepsilon}}{n_e n_1 x \, R_o^x} \right]^{I/x} \tag{19}$$

Solving Eq (13) for n_e and applying the breakdown criterion yields

$$t_1 = \frac{\ln(n_e^1/n_e^o)}{n_1 R_o^I} \left[\frac{e^2 S \nu}{n_1 x \, R_o^x m_e c \, {}_o(\nu^2+\omega^2)} \right]^{I/x} \tag{20}$$

which is Eq (2) with $\tau = 1/n_1\langle R^I \rangle$, and replaced by Eq (9). Thus, for a given laser intensity S, breakdown will occur only if the laser pulse length meets the criterion of Eq (20).

The conditions under which the assumption of a temperature is valid will be discussed later in this report (Chapter IV.)

The Quantum Kinetic Equation

The classical electron heating rate of Eq (9) was originally derived for use in microwave breakdown studies and assumes a continuous absorption of energy by the electron. At microwave frequencies this assumption is valid since the energy of each photon is small, and the average energy per collision absorbed by an electron(as calculated by Eq 9) is many times the energy of a single photon. At optical frequencies the energy of a photon becomes appreciable and the average energy per collision absorbed by an electron is only a small fraction of the energy of a single photon. Thus, an electron will experience many collisions which do not involve the absorption of energy and a quantum mechanical approach should be taken(Ref 3:657).

The heating of electrons by the radiation is the net result of two competing processes. The first, bremsstrahlung absorption, occurs when an electron absorbs a photon from the radiation field during collisions with atoms or ions. The second, bremsstrahlung emission, occurs when an electron is stimulated by the radiation field to emit a photon upon collision with an atom or ion. A coefficient of bremsstrahlung absorption can be derived quantum mechanically and is given by(Ref 6:540)

$$a(\epsilon) = \frac{2e^2}{3m_e c \epsilon_o \omega^2}\left[\frac{2(\epsilon + \hbar\omega)}{m_e}\right]^{1/2}\frac{(\epsilon + \hbar\omega/2)}{\hbar\omega}\,\sigma_m(\epsilon + h\omega/2) \qquad (21)$$

where ϵ is the electron energy, $\hbar\omega$ is the energy of the photon absorbed, and σ_m is the momentum transfer cross section of the electron-atom pair. A coefficient of bremsstrahlung emission can be obtained from Eq (21) using microreversibility (Ref 2:774)

$$b(\epsilon + \hbar\omega) = a(\epsilon)\left[\frac{\epsilon}{\epsilon + \hbar\omega}\right]^{1/2} \qquad (22)$$

Now, if the quantum mechanical rates for bremsstrahlung emission and absorption are used to replace the microwave heating term in Eq (10) the resulting quantum kinetic equation will be

$$\begin{aligned}\frac{\partial f(\epsilon)}{\partial t} = {} & Fn_a\{a(\epsilon - \hbar\omega)f(\epsilon - \hbar\omega) - [a(\epsilon) + b(\epsilon)]f(\epsilon) \\ & + b(\epsilon + \hbar\omega)f(\epsilon + \hbar\omega)\} - \sum_{i,j>i} n_i R^x_{ij}(\epsilon)f(\epsilon) \\ & + \sum_{i,j>i} n_i R^x_{ij}(\epsilon + x_{ij})f(\epsilon + x_{ij}) - \sum_j n_j R^I_j(\epsilon)f(\epsilon) \\ & + \sum_j n_j R^I_j(\epsilon + I_j)f(\epsilon + I_j) \\ & + \delta(\epsilon)\sum_j n_j \int_0^\infty R^I_j(\epsilon)f(\epsilon)d\epsilon \end{aligned} \qquad (23)$$

where F is the photon flux(#/cm^2-sec) and n_a is the total

number of atoms. The first term on the right hand side of Eq (23) is the rate at which electrons of energy ϵ are gained as a result of bremsstrahlung absorption and emission.

A Diffusion Model

As previously mentioned the heating of the electrons by a laser can be viewed as a diffusion of electrons along the energy axis. This approach was originally presented by Zeldovich and Raizer(Ref 2). Eq (23) can be rewritten in the form

$$\frac{\partial f(\epsilon)}{\partial t} = Fn_a \left\{ a(\epsilon - \hbar\omega) f(\epsilon - \hbar\omega) - \left[a(\epsilon) + b(\epsilon) \right] f(\epsilon) + b(\epsilon + \hbar\omega) f(\epsilon + \hbar\omega) \right\} + Q \qquad (24)$$

where Q includes all electron energy gain and loss mechanisms not specifically written out. In the region near the excitation and ionization energies $\hbar\omega/\epsilon$ is a small quantity and the bremsstrahlung absorption and emission terms can be expanded in a Taylor series in powers of $\hbar\omega/\epsilon$. Retaining terms to second order results in (Ref 2:775)

$$\frac{\partial f(\epsilon)}{\partial t} = - \frac{\partial J}{\partial \epsilon} + Q \qquad (25)$$

$$J = - D \frac{\partial f(\epsilon)}{\partial \epsilon} + uf(\epsilon) \tag{26}$$

where $$D = \frac{1}{2} Fn_a(\hbar\omega)^2 \left[a(\epsilon) + b(\epsilon)\right] \tag{27}$$

and $$u = Fn_a\hbar\omega\left[a(\epsilon) - b(\epsilon)\right] - \frac{\partial D}{\partial \epsilon} \tag{28}$$

Eqs (25)-(26) represent a diffusion of electrons along the energy axis. D is the diffusion coefficient, u is the net velocity of the electrons along the energy axis, and Q represents an electron "source". Eqs (27)-(28) can be simplified further by expanding $b(\epsilon)$ in terms of $\hbar\omega/\epsilon$ yielding(Ref 2:775)

$$D = Fn_a(\hbar\omega)^2 a(\epsilon) \tag{29}$$

$$u = \frac{D}{2\epsilon} \tag{30}$$

If Q is assumed to be zero (no sources), Eq (25) can be multiplied by ϵ and integrated over all energy so that in the limit as $\hbar\omega/\epsilon \rightarrow 0$ it becomes(Ref 2:776)

$$\frac{d\langle\epsilon\rangle}{dt} = \frac{e^2 S \nu}{m_e c \epsilon_o \omega^2} \tag{31}$$

where ν was defined to be $n_a v \sigma_m$. At optical frequencies $\nu^2 \ll \omega^2$, and Eq (31) agrees with Eq (9) which gives the classically defined electron heating rate. Thus, it can be seen that the quantum kinetic model reduces to the

correct classical limit as $\hbar\omega/\epsilon \rightarrow 0$, and for $\hbar\omega/\epsilon$ small the classical heating rate, $\dot{\epsilon}$, can be used to accurately describe the net bremsstrahlung absorption of laser radiation.

The exact method of solution of Eq (25) is not important, but the results does have a natural physical interpertation which should be discussed. Q, in Eq (25), can be replaced by a boundary condition involving the probability of ionization. The electrons are then assumed to increase in energy until they reach I_a, an energy 1-3 eV greater than the ionization potential. Having reached this energy the electrons will lose their energy to ionization with a probability α and to excitation with a probility $1-\alpha$. Under these conditions Eq (25) can be solved for the cascade time constant(Ref 2:777)

$$\tau = t_a/\alpha \tag{32}$$

where $t_a = I_a/3u$ is the time it takes an electron to grow in energy from 0 to I_a, and $1/\alpha$ represents the number of times this cycle must be repeated before an ionization occurs. Thus, the electron growth rate, $R = 1/\tau$, depends on the laser flux through t_a and on the properties of the gas through α. This is consistent with the results of the temperature model.

III. Approach

If a comparison of the results of a temperature model with those of the more accurate quantum kinetic model is to be valid care must be taken to insure that each model is solved under similar conditions. The first part of this chapter discusses the various assumptions made to develop self consistent models. The remainder of the chapter outlines the solution of the models and the comparisons made.

The Model Atom

The gas upon which the laser energy is incident consists of a single atomic species. The atom has a mass of 15 amu and consists of a core and one electron. Three energy levels are permitted: a ground state at -14 eV, a first excited state at -3.5 eV, and a second excited state at -1.54 eV. Ionizations can occur from any state and transitions are allowed between any two levels. Multiple ionizations of an atom are ignored. The temperature of the gas (atoms and ions) is assumed to remain constant until late in the cascade when heating by the electrons becomes significant.

Cross Sections and Rates

Cross sections and rates for the various processes involved in breakdown were either chosen or calculated so as to insure complete correspondence between the quantum

kinetic rate and its temperature model counterpart. The quantum kinetic rates for ionization and excitation were determined using analytic formulas

$$R(\epsilon) = \sqrt{\frac{2\epsilon}{m_e}}\,\sigma(\epsilon) \tag{33}$$

where $\sigma(\epsilon)$ is the cross section for either ionization or excitation. Substituting the ionization cross section into Eq (33) yields(Ref 5:392)

$$R_j^I(\epsilon) = \sqrt{\frac{2}{m_e}}\,\frac{\pi e^4}{(4\pi\epsilon_o)^2}\,\frac{1}{I_j}\,\epsilon^{-3/2}(\epsilon - I_j) \qquad \epsilon \geq I_j \tag{34}$$

where R_j^I is the ionization rate for the jth level and I_j is the corresponding ionization energy. In a similar manner an excitation rate can be obtained(Ref 5:396)

$$R_{ij}^x(\epsilon) = \sqrt{\frac{2}{m_e}}\,\frac{\pi e^4}{(4\pi\epsilon_o)^2}\,\frac{1}{x_{ij}}\,3f_{ij}\,\epsilon^{-3/2}(\epsilon - x_{ij}) \qquad \epsilon \geq x_{ij} \tag{35}$$

where R_{ij}^x is the excitation rate from level i to level j, x_{ij} is the excitation energy, and f_{ij} the oscillator strength for absorption. As can be seen from Fig 1 these analytic rates compare favorably with similar data obtained experimentally(Ref 7:115).

The corresponding temperature model rates were obtained by multiplying the quantum kinetic rates by a Maxwell-Boltzmann distribution function and integrating over all energy. The ionization rate is

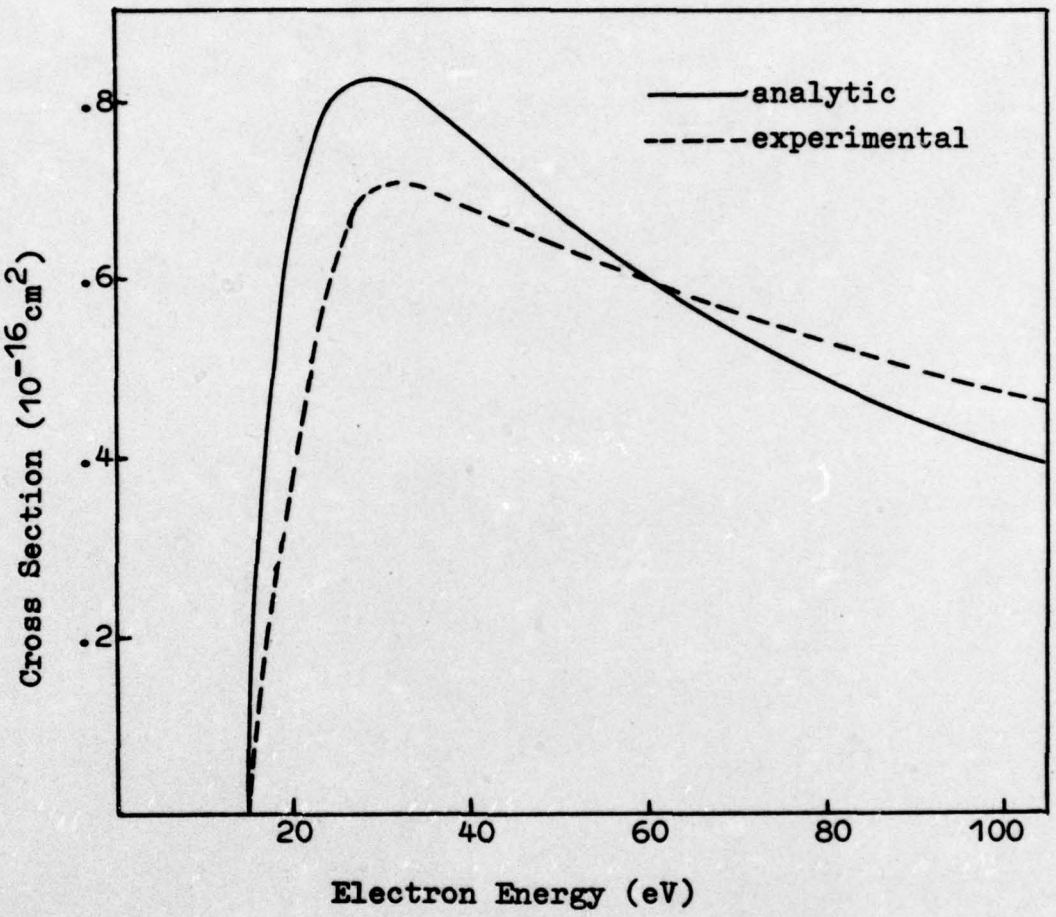

Fig. 1 Cross Section for Ionization

$$R_j^I(T) = \frac{2^{3/2}\sqrt{\pi}e^4}{\sqrt{m_e}(4\pi\epsilon_o)^2 I_j} \frac{1}{T^{1/2}} \left[e^{-I_j/T} + E_i(-I_j/T)\right] \qquad (36)$$

where E_i is a tabulated integral defined by

$$E_i(x) = \int_{-\infty}^{x} \frac{e^t}{t}\, dt \qquad (37)$$

Similarly, the excitation rate is given by

$$R_{ij}^x(T) = \frac{2^{3/2}\sqrt{\pi}e^4 3 f_{ij}}{\sqrt{m_e}(4\pi\epsilon_o)^2 x_{ij}} \frac{1}{T^{1/2}} \left[e^{-x_{ij}/T} + \frac{x_{ij}}{T} E_i(-x_{ij}/T)\right] \qquad (38)$$

A complete treatment of the above cross sections and rates, along with a table of numerical formulas, can be found in Appendicies A and B. Rates for deexcitation and recombination were not computed since they were ignored in the solution of the equations.

Finally, a value for the electron-atom momentum transfer cross section, $\sigma_m = 7.1 \times 10^{-16} cm^2$, was taken from Brown(Ref 7:5). This cross section is used to compute the value of ν in Eq (9) and also to compute $a(\epsilon)$ in Eq (21). A cross section for electron-ion collisions was not calculated since electron-ion collisions were ignored.

The Quantum Kinetic Model

For the three level model atom assumed the quantum kinetic equation can be written as

$$\frac{\partial f(\epsilon)}{\partial t} = Fn_a \{a(\epsilon - \hbar\omega)f(\epsilon - \hbar\omega) - [a(\epsilon) + b(\epsilon)]f(\epsilon) + b(\epsilon + \hbar\omega)f(\epsilon + \hbar\omega)\} - \sum_{i,j>i} n_i R^x_{ij}(\epsilon)f(\epsilon) + \sum_{i,j>i} n_i R^x_{ij}(\epsilon + x_{ij})f(\epsilon + x_{ij}) - \sum_j n_j R^I_j(\epsilon)f(\epsilon) + \sum_j n_j R^I_j(\epsilon + I_j)f(\epsilon + I_j) + \delta(\epsilon) \sum_j n_j \int_0^\infty R^I_j(\epsilon)f(\epsilon)d\epsilon \quad (23)$$

The first term on the right side of Eq (23) represents the rate at which electrons of energy ϵ are gained as a result of bremsstrahlung absorption and emission. The coefficients a and b are given by Eqs (21)-(22); F is the photon flux(#/cm^2-sec) and n_a is the total number of atoms (#/cm^3). The next two terms of Eq (23), involving R^x_{ij}, represent the rate at which electrons of energy ϵ are lost as a result of excitations. The summation over i goes from 1 to 3 and the R^x_{ij} are given by Eq (35). The fifth and sixth terms of Eq (23) represent the rate at which electrons of energy ϵ are lost as a result of ionizations. The summation over j goes from 1 to 3 and the R^I_j are given by Eq (34). Finally, the last term of

Eq (23) represents the rate at which electrons with zero energy are created by ionizations from each of the three atomic levels.

There are several assumptions implicit in Eq (23) that should be mentioned. First, the diameter of the incident laser beam is assumed to be large(~ 1 cm). Diffusion of electrons from the region of the beam's action will then be minimal($\tau_D \sim 10^{-6}$ sec) and can be neglected. During the early portion of the cascade, electron-ion collisions will be rare and can be neglected. This eliminates the need to consider the bremsstrahlung heating of electrons by ions, and triple body recombination resulting from the collision of an ion and two electrons. For a similar reason, electron-electron collisions can be ignored. Finally, the deexcitation of atoms is neglected. The energy lost to deexcitations is very small and the rate of ionization from the excited states is not strongly affected.

Besides Eq (23), three other equations contribute to the quantum kinetic description of breakdown. These are the equations governing the change in the population of the three atomic levels

$$\frac{dn}{dt}1 = -n_1 n_e\left[\langle R_1^I(\epsilon)\rangle + \langle R_{12}^x(\epsilon)\rangle + \langle R_{13}^x(\epsilon)\rangle\right] \qquad (39)$$

$$\frac{dn}{dt}2 = n_1 n_e\langle R_{12}^x(\epsilon)\rangle - n_2 n_e\left[\langle R_2^I(\epsilon)\rangle + \langle R_{23}^x(\epsilon)\rangle\right] \qquad (40)$$

$$\frac{dn_3}{dt} = n_1 n_e \langle R^x_{13}(\epsilon)\rangle + n_2 n_e \langle R^x_{23}(\epsilon)\rangle - n_3 n_e \langle R^I_3(\epsilon)\rangle \qquad (41)$$

where $\langle R(\epsilon)\rangle$ is the energy average of the corresponding rate. These equations together with Eq (23) can now be solved numerically using methods similar to those of Ref 8 (see Appendix D). It should be noted that a good estimate of the cascade growth rate can be obtained by solving Eq (23) independent of Eqs (39)-(41) using the initial values of n_1, n_2, n_3. However, Eqs (39)-(41), as well as other effects, become important if a solution is to be carried to breakdown.

The Temperature Model

In an effort to insure self-consistency, the temperature model equations are obtained directly from the quantum kinetic equations. For $\hbar\omega/\epsilon$ assumed small, the bremsstrahlung absorption and emission terms in Eq (23) can be replaced by the microwave heating term, Eq (9). The electron distribution function, an unknown in Eq (23), is assumed to be maxwellian

$$f(\epsilon) = \frac{2}{\sqrt{\pi}} \frac{\epsilon^{1/2}}{T^{3/2}} e^{-\epsilon/T} \qquad (42)$$

If Eq (23), as modified, is integrated over all energy the zeroth energy moment of the Boltzmann equation will result

$$\frac{dn_e}{dt} = n_e \sum_j n_j \langle R_j^I \rangle \tag{43}$$

where the $\langle R_j^I \rangle$ are now averages over a maxwellian, and are a function of temperature. Eq (43) describes the rate of growth of free electrons. Eq (23) can also be multiplied by ϵ and integrated over all energy to obtain the first energy moment of the Boltzmann equation

$$\frac{d\langle\epsilon\rangle}{dt} = \frac{\dot{\varepsilon}}{n_e} - \sum_j n_j I_j \langle R_j^I \rangle$$

$$- \sum_{i,j>i} n_i x_{ij} \langle R_{ij}^x \rangle - \frac{\langle\epsilon\rangle}{n_e} \frac{dn_e}{dt} \tag{44}$$

where $\langle\epsilon\rangle = (3/2)T$ is the average electron energy. Eq (44) describes the rate of growth of the average free electron energy. To complete the description of the temperature model Eqs (39)-(41) must be included with Eqs (43)-(44). The rates in these equations are all functions of temperature and are the result of averaging over a maxwellian. A more complete derivation of the temperature model can be found in appendix C.

The assumptions involved in the temperature model are identical with those of the quantum kinetic model with two exceptions. The bremsstrahlung emission and absorption terms were replaced by a microwave heating term. For $\hbar\omega/\epsilon$ small the two terms will yield the same electron heating rate so that consistency is maintained. The second excep-

tion involves electron-electron collisions. If the maxwellian nature of the electron distribution is to be maintained, electron-electron collisions must be at least implicitly allowed. Since it is the validity of the assumption of a maxwellian that is being tested, this will not cause a conflict.

The temperature model equations are solved numerically using a procedure outlined in appendix E.

Solution and Comparison

The two breakdown models have been solved under a variety of conditions to obtain a comparison of the results and behavior of each model. Certain initial conditions were imposed and remained fixed for all comparisons. The laser radiation was assumed to have a wavelength of 10.6μ. This fixes the energy of a photon at .12 eV. The initial density of ground state atoms was assumed to be $2.5 \times 10^{19}/cm^3$. The initial temperature of the gas was set at .1 eV. This condition fixed the initial population density of the first and second excited states as well as the total number of atoms initially present. The cascade was assumed to proceed from an initial free electron density of $100/cm^3$. Since solution of the quantum kinetic model requires that the energy axis be divided into bins(see appendix D), a standard of 25-1eV bins was chosen.

Under these conditions the two models were solved utilizing the rates found in table X(Appendix B). The

cascade growth rates predicted by each model were computed for a wide range of incident flux densities($5 \times 10^7 - 10^{12}$ W/cm^2) and compared. A study of the apportionment of energy among the various loss mechanisms suggested that a comparison of the growth rates predicted by the two models be performed assuming a two level atom. Finally, the results of the quantum kinetic model were compared for various bin widths.

To determine the effects of manipulation of energy levels and ionization and excitation rates, comparisons of the growth rates were made under the following conditions:

1. R_{12}^x increased by a factor of 10.
2. R_{12}^x decreased by .5
3. R_1^I increased by a factor of 10.
4. R_1^I decreased by .5
5. Ground state energy raised to -13 eV.
6. Ground state energy lowered to -15 eV.
7. 1st excited state energy raised to -2.5 eV.
8. 1st excited state energy lowered to -4.5 eV.

The results of all comparisons performed will be discussed in Chapter IV.

An Improved Diffusion Model

In an attempt to find a breakdown model applicable over a wider range of incident fluxes, the improved diffusion model of Vyskrebentsev and Raizer(Ref 9) was studied. Unlike the old model of Zeldovich and Raizer,

excitations are treated specifically rather than being lumped into a generalized term, Q. Assuming a two level atom, Eq (25) can be modified to(Ref 9:33)

$$\frac{\partial f(\epsilon)}{\partial t} = - \frac{\partial J}{\partial \epsilon} - h(\epsilon) f(\epsilon) \nu^* \tag{45}$$

where

$$h(\epsilon) = \begin{cases} 0 \text{ for } \epsilon < x_a \\ 1 \text{ for } x_a \leq \epsilon < I_a \end{cases} \tag{46}$$

The energy x_a is defined to be approximately 1eV greater than the excitation energy, x, while I_a is 1eV greater than the ionization energy, I. In the interval from x_a to I_a, the average excitation rate, ν^*, is assumed constant.

Eq (45) can be solved with the aid of several boundary conditions. At $\epsilon = x_a$, $f(\epsilon)$ and $df(\epsilon)/d\epsilon$ are assumed to be continuous. All electrons reaching I_a are assumed to lose their energy to ionization with a probability β and to excitation with a probability $(1-\beta)$ so that $f(I_a) = 0$. Finally, the rate at which electrons appear with energy zero equals the rate of excitation in the interval $x_a \leq \epsilon < I_a$, plus twice the rate of ionization(this accounts for newly born electrons). Under these conditions Eq (45) yields a transcendental equation for the cascade growth rate, ν_i(Ref 9:34),

$$e^{(a-1)y}\left[\cosh\left(\frac{y}{z}\right) + z\sinh\left(\frac{y}{z}\right)\right] - e^{-(a-1)y}\left[\cosh\left(\frac{y}{z}\right)\right.$$

$$\left. - z\sinh\left(\frac{y}{z}\right)\right] - 2a(1+\beta)y - 2(1-z^{-2})\left\{y\cosh\left[(a-1)y\right]\right.$$

$$\left. + \sinh\left[(a-1)y\right] - ay\right\} = 0 \qquad (47)$$

where
$$y = \sqrt{6(\nu_i + \nu^*)x_a/(\varepsilon/n_e)} \qquad (48)$$

$$z = \sqrt{1 + \nu^*/\nu_i} \qquad (49)$$

$$a = \sqrt{I_a/x_a} \qquad (50)$$

Before Eq (47) can be solved β, ν^*, and ε must be evaluated. The value of β is obtained from

$$\beta = \frac{R_1^I(I_a)}{R_1^I(I_a) + R_{12}^x(I_a)} \qquad (51)$$

and is found to be .09 . The rates in Eq (51) were calculated using table X(Appendix B). The value ν^* is defined by(Ref 9:33)

$$\nu^* = n_a \bar{v}^* \bar{\sigma}^* \qquad (52)$$

where $\bar{v}^*$ and $\bar{\sigma}^*$ are mean values of the electron velocity and excitation cross section in the interval $x_a < \epsilon < I_a$ determined by

$$\bar{\nu}^* = \frac{\sqrt{\frac{2}{m_e}} \int_{x_a}^{I_a} \epsilon^{1/2} f(\epsilon) d\epsilon}{\int_{x_a}^{I_a} f(\epsilon) d\epsilon} \tag{53}$$

$$\bar{\sigma}^* = \frac{\sqrt{\frac{2}{m_e}} \int_{x_a}^{I_a} \epsilon^{-1/2} R_{12}^{x}(\epsilon) d\epsilon}{I_a - x_a} \tag{54}$$

for $n_a = 2.5 \times 10^{19}/cm^3$ Eqs (52)-(54) yield a value for ν^* of 8.5×10^{11}/sec. The quantity $\dot{\epsilon}$ is evaluated over a range of fluxes using Eq (9). Eq (47) can then be solved numerically and the growth rates compared with corresponding quantum kinetic rates.

A Two-Temperature Model

Analysis of the results of the comparisons between the temperature model and the quantum kinetic model(Chapter IV) suggested that modification of the temperature model distribution function might lead to a more accurate prediction of the growth rate. The most encouraging approach appeared to be one in which the electron distribution function was broken into two sections, each described by a different temperature.

The problem is first simplified by considering a two level atom. The two-temperature electron distribution function is then defined as

$$f(\epsilon) = \begin{cases} C_1 \epsilon^{1/2} e^{-\epsilon/T_1} & \text{for } 0 \le \epsilon \le x \\ C_2 \epsilon^{1/2} e^{-\epsilon/T_2} & \text{for } x \le \epsilon < \infty \end{cases} \tag{55}$$

where x is the excitation energy of the model atom. This distribution function is assumed to be continuous at the boundary of the two regions

$$C_1 e^{-x/T_1} = C_2 e^{-x/T_2} \tag{56}$$

A second condition requires that the distribution function be normalized

$$C_1 \int_0^x \epsilon^{1/2} e^{-\epsilon/T_1} \, d\epsilon + C_2 \int_x^\infty \epsilon^{1/2} e^{-\epsilon/T_2} \, d\epsilon = 1 \tag{57}$$

The energy balance equation of the old temperature model is also needed

$$\frac{d\langle\epsilon\rangle}{dt} = \frac{\dot{\epsilon}}{n_e} - x\langle R^x \rangle n_1 - I\langle R^I \rangle n_1 - \frac{\langle\epsilon\rangle}{n_e} \frac{dn_e}{dt} \tag{14}$$

It should be noted that the average energy and the rates in this equation must be reevaluated using the modified distribution function defined in Eq (55). Assuming a rapid equilibration of the average electron energy and substituting for dn_e/dt using Eq (13) the energy balance equation becomes

$$\frac{\dot{\epsilon}}{n_e} - xn_1\langle R^x\rangle - (I + \langle\epsilon\rangle)n_1\langle R^I\rangle = 0 \qquad (58)$$

Eqs (56)-(58) form a set of three equations in four unknowns. A fourth condition on the unknowns can be obtained by taking the second energy moment of the Boltzmann equation(Appendix F). This will yield an equation for the time rate of change of $\langle\epsilon^2\rangle$

$$\frac{d\langle\epsilon\rangle}{dt} = 2\frac{\dot{\epsilon}}{n_e}\langle\epsilon\rangle + x^2n_1\langle R^x\rangle + I^2n_1\langle R^I\rangle$$

$$- 2xn_1\langle\epsilon R^x\rangle - 2In_1\langle\epsilon R^I\rangle = \frac{\langle\epsilon^2\rangle}{n_e}\frac{dn_e}{dt} \qquad (59)$$

where the averages must be taken over the distribution function defined by Eq (55). Again, assuming a rapid equilibration of $\langle\epsilon^2\rangle$ and using Eq (13) yields

$$2\frac{\dot{\epsilon}}{n_e}\langle\epsilon\rangle + x^2n_1\langle R^x\rangle + (I^2 - \langle\epsilon^2\rangle)n_1\langle R^I\rangle$$

$$-2xn_1\langle\epsilon R^x\rangle - 2In_1\langle\epsilon R^I\rangle = 0 \qquad (60)$$

The two-temperature model consisting of Eqs (56)-(58) and (60) can now be solved. The initial conditions used were identical to those used in solving the quantum kinetic model. To obtain a solution the constants C_1 and C_2 are first eliminated from Eqs (58) and (60) using Eqs (56) and (57). Eqs (58) and (60) must then be solved numeri-

cally for the values of T_1 and T_2. The two constants can then be determined by substituting for T_1 and T_2 in Eqs (56) and (57). The cascade growth rate, $n_1\langle R^I\rangle$, is calculated using

$$n_1\langle R^I\rangle = n_1 C_2 \int_I^\infty \epsilon^{1/2} R^I(\epsilon) e^{-\epsilon/T_2}\, d\epsilon \qquad (61)$$

and compared with the corresponding quantum kinetic rate.

Comparisons were made under two sets of conditions. First, Eqs (59) and (60) were solved approximately by assuming that most of the energy went into excitations. The third term in Eq (58) and the third and fifth terms in Eq (60) could then be neglected. Also, $\langle\epsilon\rangle$ was assumed to be $(3/2)T_1$. The equations were then resolved without any approximations(Appendix G). Results of the comparisons will be discussed in Chapter IV.

IV. Analysis and Discussion

The results of each of the comparisons will be presented and discussed in this chapter. All comparisons were made during the early portion of the electron cascade, shortly after a steady state had been established. The first portion of the chapter discusses the results of the temperature model comparisons. The remainer of the chapter will deal with the comparisons involving the improved diffusion model and the two temperature model.

The Temperature Model

The comparisons between the temperature model and the quantum kinetic model were made at several values of incident laser flux ranging from 5×10^{7}-10^{12} W/cm^2. The results of these comparisons are presented in figs. 2 - 4 and table I. Fig. 2 is a plot of the cascade growth rate as a function of flux for both the quantum kinetic and temperature models. Figs. 3 and 4 are plots of the electron distribution functions predicted by both models at 5×10^{8} W/cm^2 and 10^{11} W/cm^2 respectively. Table I summarizes the apportionment of energy among the various loss mechanisms for several values of incident flux.

A comparison of the growth rates predicted by each of the models can be made from fig. 2. At higher fluxes, those above 5×10^{9} W/cm^2, the rates predicted by the temperature model agree rather well with the quantum kinetic

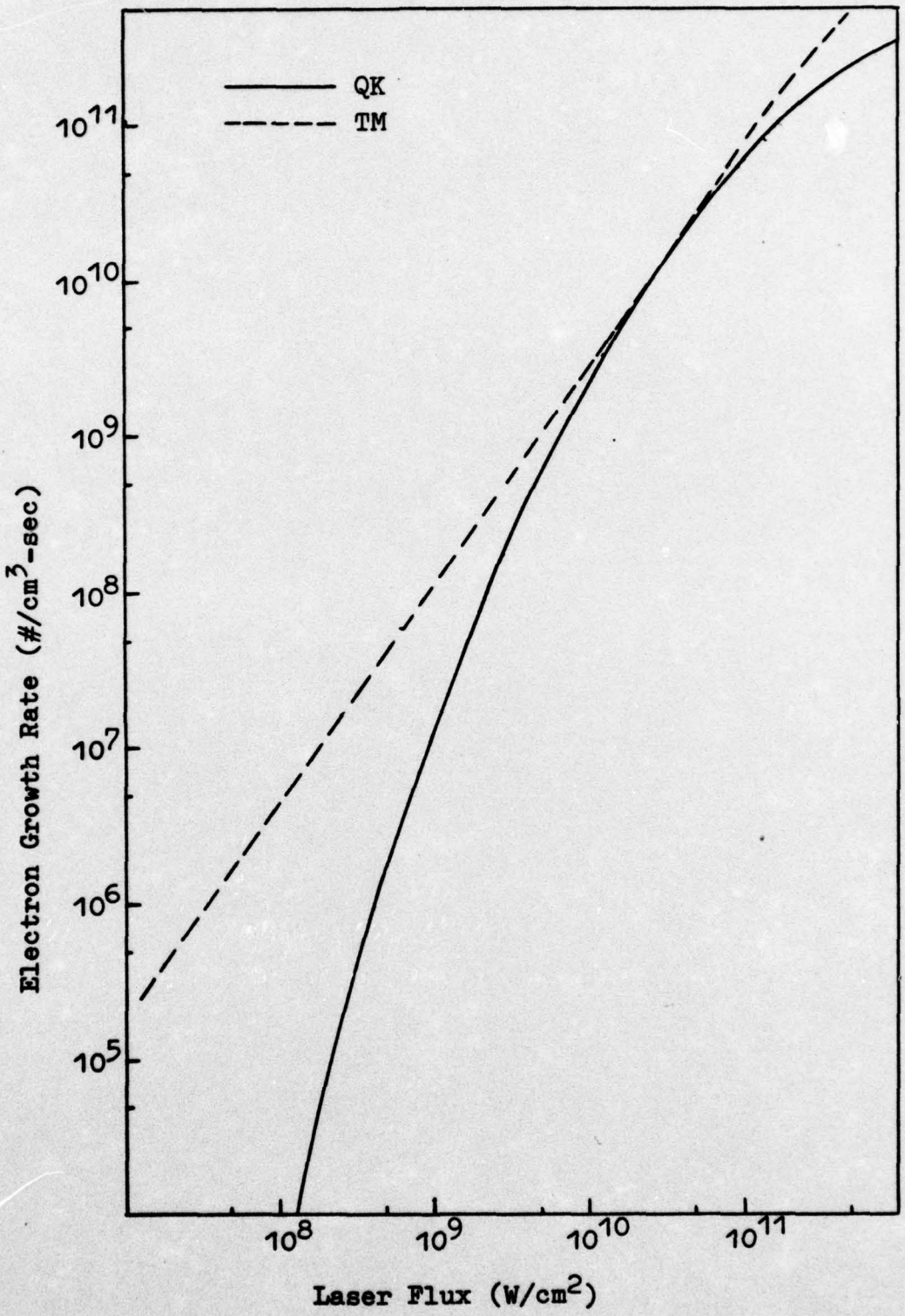

Fig. 2 Electron Growth Rate

rates. Below $5 \times 10^9 W/cm^2$ the predictions of the two models begin to diverge, disagreeing by more than four orders of magnitude at $5 \times 10^9 W/cm^2$. The rates predicted by the temperature model are much too large. This suggests that at lower fluxes a maxwellian distribution function permits too many electrons of higher energy to exist. This can be confirmed using fig. 3 which plots the two distribution functions for an incident flux of $5 \times 10^8 W/cm^2$. At energies above 14 eV, the ionization energy of the ground state, the quantum kinetic distribution function predicts an electron density significantly smaller than that of the temperature model. Fewer electrons are therefore available for ionizations and a lower growth rate results. In the region between 10.5 eV, the ground state excitation threshold, and 14 eV the situation is reversed. The electron density of the quantum kinetic model is now greater than that of the temperature model. Thus, not only does the temperature model predict an excessively high growth rate, but it also permits fewer excitations than the quantum kinetic model. Finally, below approximately $1.5 \times 10^8 W/cm^2$ the quantum kinetic growth rate becomes small enough that many of the neglected processes become important. If these are taken into account, the quantum kinetic growth rate would be reduced and breakdown might not occur. However, the temperature model rate would remain unaffected and erroneously predict breakdown at fluxes well below the breakdown threshold.

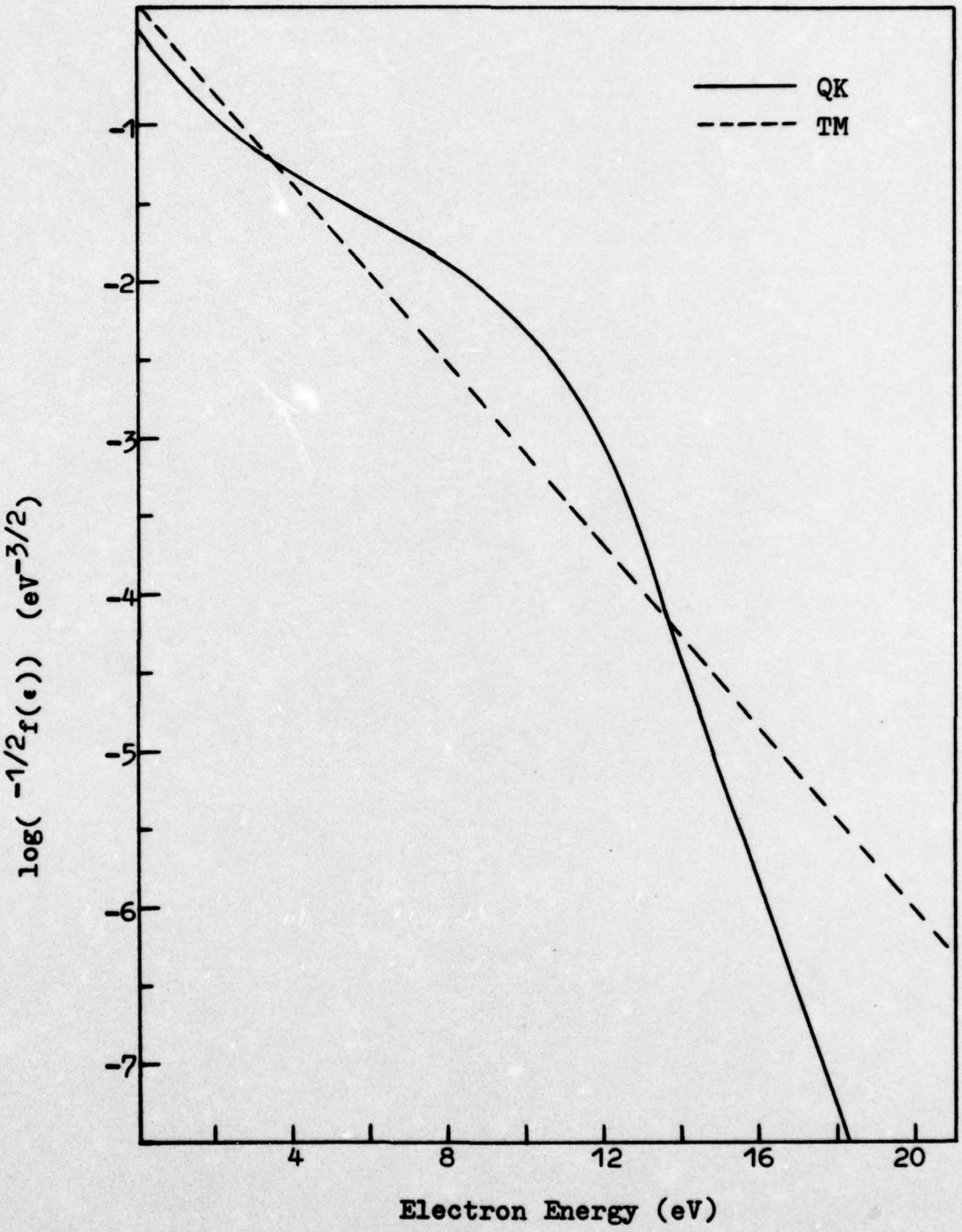

Fig. 3 Electron Distribution at $5x10^8 W/cm^2$

Focusing attention on the high fluxes, it can be seen that the quantum kinetic curve of fig. 2 begins to diverge from the temperature model curve above $10^{11} W/cm^2$. Closer study revealed that this divergence was artificially created by the conditions under which the quantum kinetic model was solved. At sufficiently high values of incident flux a sizable number of electron will possess energies in excess of 25 eV; however, the procedure used to obtain a numerical solution limits electrons to a maximum energy of 25 eV. Solution of the quantum kinetic model using 30, 40, and 50 1-eV bins produced improved rates. As the number of bins was increased, the quantum kinetic rates approached those of the temperature model. The effects of bin size on the quantum kinetic rates was also investigated. An increase to 2 eV and 3 eV bins resulted in a significant increase in the growth rates while reducing the bin size to .75 eV and .5 eV had little effect on the rates. Therefore, the choice of 1 eV bin size appears to be justified.

An analysis of the energy gain and loss mechanisms can be made using table I. The rate (eV/sec) at which an electron absorbs energy from the radiation field is given by $\dot{\varepsilon}$. The losses due to the different mechanisms are given as a percentage of the energy gained. Losses which result from ionization out of the second and third levels, and excitations between these levels are not included since these losses are 10 - 15 orders of magnitude smaller

Table I

Apportionment of Energy Losses
(Losses given as a % of $\dot{\varepsilon}$)

Flux (W/cm^2)	$\dot{\varepsilon}$ (eV/sec)		R_1^I		R_{12}^x		R_{13}^x		ε_T	
	QK	TM	QK	TM	QK	TM	QK	TM	QK	TM
5×10^7	2.21×10^9	1.31×10^9	-	1.9	100	95.2	.001	2.6	-	.2
10^8	4.49×10^9	2.73×10^9	.001	2.3	99.8	94.5	.2	2.9	-	.3
5×10^8	2.41×10^{10}	1.51×10^{10}	.09	3.8	99.1	92.0	.8	3.7	.02	.5
10^9	5.03×10^{10}	3.18×10^{10}	.39	4.8	97.4	90.1	1.6	4.3	.7	.8
5×10^9	2.82×10^{11}	1.84×10^{11}	3.7	7.8	91.0	85.0	4.2	5.4	1.1	1.8
10^{10}	5.94×10^{11}	3.97×10^{11}	6.5	9.6	86.1	81.8	5.4	6.0	2.0	2.6
5×10^{10}	3.01×10^{12}	2.55×10^{12}	13.5	14.7	73.2	71.5	7.1	7.2	6.2	6.6
10^{11}	6.83×10^{12}	6.04×10^{12}	18.0	17.2	63.3	64.5	7.5	7.5	11.2	10.8

than the others and need not be considered.

The energy gain rates predicted by the two models agree reasonably well over the entire range of incident fluxes. This is to be expected since the classical microwave heating rate used in the temperature model was derived directly from the quantum kinetic rate for net bremsstrahlung absorption(Appendix C). Although the two rates are independent of their respective distribution functions, the small difference in the rates can be attributed to the different average energies predicted by the two models(see table II).

Table II

Average Electron Energy (eV)

Flux (W/cm^2)	$\langle \epsilon \rangle$	
	TM	QK
5×10^7	1.65	2.84
10^8	1.80	2.93
5×10^8	2.25	3.29
10^9	2.45	3.53
5×10^9	3.26	4.34
10^{10}	3.81	4.86
5×10^{10}	6.30	6.90
10^{11}	8.84	9.41

At fluxes above $5 \times 10^9 W/cm^2$ the two models agree rather well in their predictions of energy lost to ground state ionization, R_1^I. However, at fluxes below 5×10^9 W/cm^2 the predictions of the two models begin to diverge, with the temperature model predicting a significantly larger loss to ionization than the quantum kinetic model. This supports an earlier conclusion, made on the basis of fig. 3, that at lower fluxes the temperature model allows too many electrons of higher energy to exist. Additional support can be found by analyzing ε_T, the energy required to bring newly born electrons into the distribution at the average energy. At lower fluxes the larger temperature model growth rate requires a much larger ε_T than does the quantum kinetic rate. This in spite of the fact that the average quantum kinetic energy is larger than the average temperature model energy(see table II).

It can be seen from table I that relatively little energy is lost to excitations between the first and third atomic levels, R_{13}^x. This suggests that the third atomic level might be eliminated with negligible effect on the growth rate. Table III summarizes the cascade growth rates predicted for both a two level and three level atom. The growth rates for the two level atom were obtained under the same conditions as those for the three level atom. The results indicate an increase in the growth rates as might be expected. However, the increases are small enough that the third level can be neglected in most calculations.

Table III

Cascade Growth Rates for
Two and Three Level Atoms

Flux	TM		QK	
	2	3	2	3
10^8	4.65×10^6	4.46×10^6	2.94×10^3	2.51×10^3
5×10^8	4.37×10^7	4.14×10^7	1.66×10^6	1.44×10^6
5×10^9	1.11×10^9	1.02×10^9	7.76×10^8	6.86×10^8
5×10^{10}	2.98×10^{10}	2.68×10^{10}	2.94×10^{10}	2.70×10^{10}
10^{11}	8.32×10^{10}	7.40×10^{10}	5.71×10^{10}	5.36×10^{10}

Referring again to table I, the energy loss to excitations between the ground state and second atomic level, R^x_{12}, can be analyzed. At the higher fluxes the two models once again predict similar losses. However, at lower fluxes the temperature model predicts a smaller excitation loss than the quantum kinetic model. In both models, excitations are the principal loss mechanism and account for up to 90 - 100% of the energy loss at lower fluxes. Thus, the lower excitation losses predicted by the temperature model allow much more energy to be available for ionizations and increased growth rates result.

Finally, the energy balance equation can be rewritten as

$$R = \frac{\dot{\epsilon}}{n_e I_1} - \frac{x_{12}}{I_1}\langle R^x_{12}\rangle n_1 \qquad (62)$$

where a two level atom was assumed and R is the cascade growth rate. From Eq (62) it can be seen that as long as the energy lost to excitations is significant the growth rate will depend strongly on the distribution function through $\langle R_{12}^x \rangle$. Therefore if the growth rates predicted by the two models are to agree, their distribution functions must be similar. At $10^{11} W/cm^2$ fig. 4 shows the distribution functions of the two models to be quite similar and fig. 2 indicates that the predicted growth rates are almost identical. Conversely, at $5 \times 10^8 W/cm^2$ fig. 3 reveals two significantly different distribution functions and fig. 2 confirms an order of magnitude difference in the growth rates.

The results of the comparisons obtained through the manipulation of the rates and energy levels will now be discussed. Eq (19), the ground state ionization rate predicted by the temperature model, can be rewritten as

$$R = n_1 R_o^I \left[\frac{\dot{\varepsilon}}{n_e n_1 x R_o^x} \right]^{I/x} \tag{63}$$

where R is the cascade growth rate and a two level atom is assumed. Using Eq (63), the effect of the manipulations on the growth rate can be predicted in most cases. However, since Eq (63) was obtained using the temperature model, it cannot be expected to accurately predict quantum kinetic model results.

Table IV presents the results of comparisons made by

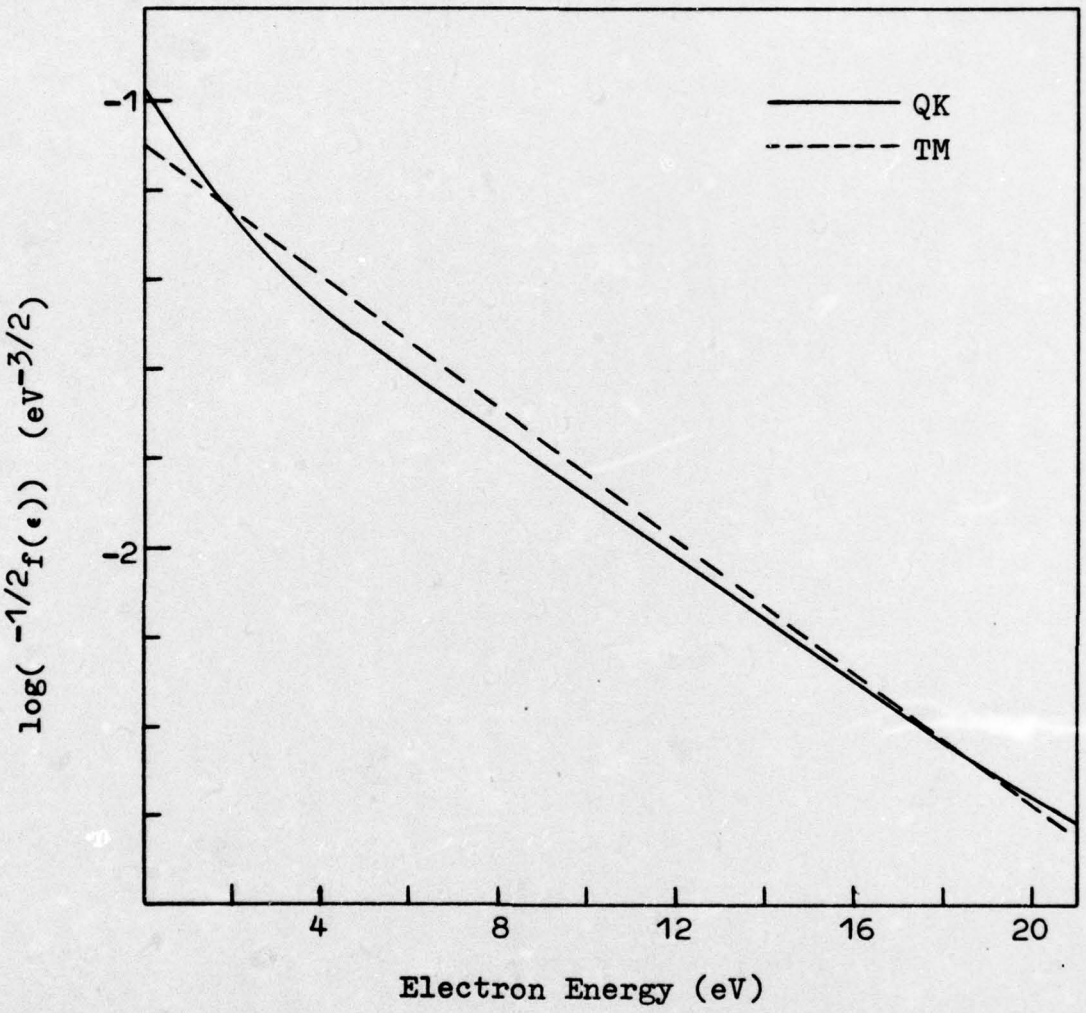

Fig. 4 Electron Distribution at 10^{11} W/cm^2

Table IV

Cascade Growth Rates at Various R_{12}^x

Flux(W/cm^2)		10^8	$5x10^8$	$5x10^9$	$5x10^{10}$	10^{11}
TM	.5 R^x	$1.07x10^7$	$9.54x10^7$	$2.16x10^9$	$4.89x10^{10}$	$1.27x10^{11}$
	R^x	$4.46x10^6$	$4.14x10^7$	$1.02x10^9$	$2.68x10^{10}$	$7.40x10^{10}$
	10 R^x	$1.95x10^5$	$1.82x10^6$	$4.62x10^7$	$1.27x10^9$	$3.52x10^9$
QK	.5 R^x	$8.31x10^6$	$1.06x10^7$	$4.02x10^9$	$6.12x10^{10}$	$9.88x10^{11}$
	R^x	$2.51x10^3$	$1.44x10^6$	$6.86x10^8$	$2.70x10^{10}$	$5.36x10^{10}$
	10 R^x	$5.57x10^{-2}$	$1.31x10^2$	$1.76x10^6$	$9.06x10^8$	$3.53x10^9$

manipulating the excitation rate, R_{12}^{x}. Eq (63) predicts that the growth rate should increase as R_{12}^{x} decreases and decrease as R_{12}^{x} increases. Table IV confirms this at all values of flux for both the temperature and quantum kinetic models. Eq (63) also accurately predicts the new values of the temperature model rates. A closer comparison of the rates in table IV reveals that for .5 R_{12}^{x} the predictions of the two models agree at fluxes as low as $10^{8}W/cm^{2}$, while for 10 R_{12}^{x} the rates of the two models show increased disagreement. This is not unexpected and can be explained using energy considerations. Since at lower fluxes almost all the energy is lost to excitations, a decrease of 50% in the excitation cross section will shift considerable energy into ionization. Thus, the energy balance will be similar to that which exists at higher fluxes and the growth rates, as predicted by Eq (62), will no longer be as strongly affected by small differences between the two distribution functions. At 10 R_{12}^{x} the reverse will be true. More energy will be forced into excitations and the growth rates of the two models will now disagree at fluxes up to $5 \times 10^{9}W/cm^{2}$.

The results of the comparisons involving the ionization rate, R_{1}^{I}, are found in table V. For .5 R_{1}^{I} the growth rates decrease as expected and the temperature model rates are close to the values predicted by Eq (63). For 10 R_{1}^{I} the growth rates increase, but the temperature model rates do not increase to the extent predicted by Eq (63). This

Table V

Cascade Growth Rates at Various R_1^I

Flux(W/cm^2)		10^8	$5x10^8$	$5x10^9$	$5x10^{10}$	10^{11}
TM	.5 R^I	$2.27x10^6$	$2.14x10^7$	$5.48x10^8$	$1.59x10^{10}$	$4.36x10^{10}$
	R^I	$4.46x10^6$	$4.14x10^7$	$1.02x10^9$	$2.68x10^{10}$	$7.40x10^{10}$
	10 R^I	$3.40x10^7$	$2.70x10^8$	$4.79x10^9$	$7.62x10^{10}$	$1.72x10^{11}$
QK	.5 R^I	$1.65x10^2$	$7.46x10^5$	$1.94x10^8$	$4.29x10^9$	$2.15x10^9$
	R^I	$2.51x10^3$	$1.44x10^6$	$6.86x10^8$	$2.70x10^{10}$	$5.36x10^{10}$
	10 R^I	$1.75x10^4$	$9.16x10^6$	$5.64x10^9$	$1.21x10^{11}$	$2.48x10^{11}$

happens because the increased ionization cross section permits more ionizations at lower energies and causes a corresponding decrease in the electron temperature. Since $\langle R^I \rangle$ is given approximately by $R_o^I e^{-I/T}$, the decrease in T will offset part of the increase in R_o^I. A comparison of the growth rates predicted by the two models reveals little change. At low fluxes the temperature model still predicts a considerably higher growth rate. This is to be expected since the change in the ionization cross section has little effect on the amount of energy going into excitations. At high fluxes, the agreement between the rates predicted by the two models is maintained with one exception: the quantum kinetic growth rate for .5 R_1^I at 10^{11} W/cm^2 is too low. Reducing the ionization cross section by 50% increases the number of electrons which possess energy above 14 eV. To properly account for this larger number of "high energy electrons" the quantum kinetic equation must be solved using an increased number of bins. If this is done the quantum kinetic growth rate for .5 R_1^I at $10^{11} W/cm^2$ will approach the higher temperature model rate.

A change in the ground state energy of the atom will affect the cascade growth rate through changes in both the ionization energy of the ground state and the excitation energy between the ground state and the first excited state. Table VI lists the growth rates which result when the ground state energy is changed. Eq (63) correctly

Table VI

Cascade Growth Rates at Various Values of Ground State Energy

Flux(W/cm^2)		10^8	5×10^8	5×10^9	5×10^{10}	10^{11}
TM	I_1=13	3.21×10^6	3.17×10^7	8.57×10^8	2.45×10^{10}	6.93×10^{10}
	I_1=14	4.46×10^6	4.14×10^7	1.02×10^9	2.68×10^{10}	7.40×10^{10}
	I_1=15	5.82×10^6	5.12×10^7	1.17×10^9	2.86×10^{10}	7.78×10^{10}
QK	I_1=13	8.10×10^2	6.43×10^5	5.00×10^8	2.73×10^{10}	5.89×10^{10}
	I_1=14	2.51×10^3	1.44×10^6	6.86×10^8	2.70×10^{10}	5.36×10^{10}
	I_1=15	6.75×10^3	2.80×10^6	8.76×10^8	2.56×10^{10}	4.72×10^{10}

predicts the new values of the temperature model rates. An increase in the ground state energy(I_1 = 13) produces a smaller growth rate while a decrease in the ground state energy(I_1 = 15) yields a larger rate. However, Eq (63) predicts the wrong trend for the quantum kinetic rates at 5×10^{10} and $10^{11} W/cm^2$. At these fluxes table VI shows that an increase in the ground state energy raises the growth rate rather than lowering it as predicted by Eq (63). Similarly, a decrease in the ground state energy produces a lower growth rate. At these fluxes, a significant amount of energy is lost to ionization and the assumptions which were made in deriving Eq (63) lose their validity. The change in the growth rate becomes a stronger function of I_1 and can be better predicted from Eq (62). At the lower fluxes Eq (63) is valid and predicts the correct trend of the quantum kinetic rates. Comparing the quantum kinetic and temperature model growth rates, a slight improvement in the agreement of the two models is noted for I_1=15. Conversely, setting I_1=13 produces a slightly greater disagreement between the rates of the two models. This can be explained by assuming that for a constant $\dot{\epsilon}$ the electrons diffuse along the energy axis at a constant velocity. Let t_I be the time required for an electron to attain sufficient energy(I_1) to cause an ionization; then $(1-x_1/I_1)t_I$ is the fraction of t_I during which excitations can occur without competition from ionization. Thus, a smaller value of $(1-x_1/I_1)t_I$ will

Table VII

Cascade Growth Rates at Various Values of First Excited State Energy

Flux(W/cm^2)		10^8	$5x10^8$	$5x10^9$	$5x10^{10}$	10^{11}
TM	I_2=2.5	$1.27x10^7$	$9.57x10^7$	$1.77x10^9$	$3.51x10^{10}$	$8.96x10^{10}$
	I_2=3.5	$4.46x10^6$	$4.14x10^7$	$1.02x10^9$	$2.68x10^{10}$	$7.40x10^{10}$
	I_2=4.5	$1.15x10^6$	$1.37x10^7$	$4.89x10^8$	$1.86x10^{10}$	$5.75x10^{10}$
QK	I_2=2.5	$8.90x10^4$	$1.16x10^7$	$1.47x10^9$	$3.32x10^{10}$	$6.07x10^{10}$
	I_2=3.5	$2.51x10^3$	$1.44x10^6$	$6.86x10^8$	$2.70x10^{10}$	$5.36x10^{10}$
	I_2=4.5	$3.54x10^1$	$1.04x10^5$	$2.51x10^8$	$2.06x10^{10}$	$4.57x10^{10}$

allow more energy to go into ionizations. This in turn will yield better agreement between the rates predicted by the two models.

Last to be discussed are the comparisons obtained by changing the first excited state energy. This change will affect only the excitation energy between the ground state and the first excited state. The results of the comparisons are presented in table VII. Eq (63) correctly predicts both the temperature model rates and the trend of the change in the quantum kinetic rates. An increase in the excited state energy(I_2=2.5) causes the growth rate to increase while a decrease in the excited state energy (I_2=4.5) yields a smaller growth rate. A closer comparison of the growth rates in table VII reveals that for I_2=2.5 the range of fluxes over which the two models predict similar growth rates is extended to $5 \times 10^8 W/cm^2$. For I_2=4.5 the disagreement between the two models is increased at lower fluxes, but the agreement at higher fluxes is not strongly affected. This behavior can be explained using the same reasoning that applied to changes in the ground state energy. As the excitation energy increases, the time during which excitations can occur without competition from ionization decreases. Therefore, more energy goes into ionizations leading to better agreement between the growth rates predicted by the two models.

The Improved Diffusion Model

The results of the comparisons between the quantum kinetic and temperature models clearly pointed out the need for a simple model that could predict cascade growth rates with reasonable accuracy at lower fluxes. Since Ref 9 stated that the results of the improved diffusion model were valid over a wide range of frequencies and conditions, it was hoped that this model would be able to predict the electron growth rate over a wider range of fluxes than the temperature model. Care was taken to insure that the diffusion model was solved under the same conditions as the quantum kinetic model. The quantity ν^* was found to be independent of the exact form of the distribution function used over the interval from x_a to I_a. The growth rates predicted by the diffusion model are given along with the corresponding quantum kinetic rates in table VIII.

Table VIII

Diffusion Model Growth Rates

Flux	QK	DM
5×10^8	1.44×10^6	3.90×10^4
5×10^9	6.86×10^8	2.17×10^8
5×10^{10}	2.70×10^{10}	1.28×10^{10}

At 5×10^9 and $5 \times 10^{10} W/cm^2$ the predicted diffusion rates come close to the quantum kinetic rates; however, they do

not appear to be quite as accurate as the temperature model growth rates. At $5 \times 10^8 W/cm^2$ the rate predicted by the diffusion model is two orders of magnitude less than the corresponding quantum kinetic rate. The predicted growth rate showed no improvement over the temperature model rate at the same flux. Finally, the failure of the improved diffusion model to predict the cascade growth rate at low fluxes appeared to be the result of its inability to accurately calculate the excitation rate. Since this was the same problem experienced with the temperature model, continued study of the improved diffusion model did not appear justified.

The Two-Temperature Model

The results of the comprisons between the quantum kinetic and temperature models showed that at low fluxes the actual electron distribution function could not be adequately approximated by a maxwellian. Referring back to fig. 3, it is seen that a maxwellian allows too many electrons to exist above the ionization energy and too few between the excitation and ionization energies. A close study of fig. 3 and similar plots at other low values of incident flux indicated that the actual distribution function could possibly be represented by two straight line segments. These line segments, each having a different slope, would intersect at the excitation energy (10.5 eV) and form a two-temperature distribution function. This

forms the basis for the two-temperature model described in chapter III.

Since results obtained earlier in this chapter indicate that at low fluxes most of the energy is lost to excitations it was expected that an approximate solution to the two-temperature model would give results accurate enough to yield a valid comparison. The growth rates resulting from the approximate solution of the two-temperature model are found in table IX. A comparison of the

Table IX

Two-Temperature Model Growth Rates

Flux	QK	2T
5×10^{7}	1.08×10^{2}	1.70×10^{-2}
5×10^{8}	1.44×10^{6}	4.37×10^{6}
5×10^{9}	6.86×10^{8}	7.19×10^{9}
5×10^{10}	2.70×10^{10}	2.23×10^{11}

quantum kinetic and two-temperature rates reveals that only at one flux, $5 \times 10^{8} W/cm^{2}$, does the predicted two-temperature rate approach the quantum kinetic rate. At all other fluxes, including high fluxes, the predicted two-temperature rates are not even within an order of magnitude of the quantum kinetic rates. The assumptions associated with the solution were reexamined and the assumption that $\langle \epsilon \rangle = (3/2)T_1$ was found to be in error.

Since $T_1 > T_2$, this assumption resulted in an overestimate of the average energy.

The two-temperature model was then solved exactly to reduce the possibility of further error. The resulting growth rates were, at every value of incident flux, much worse than the rates of table IX. Agreement with the quantum kinetic model growth rates did not exist nor did the rates approach those of the temperature model at high fluxes. Thus, it appears that the two-temperature model, which was based on approximating the shape of the distribution function, is not valid and the possibility that the electron distribution is a function of an additional variable, such as incident laser flux, should be considered.

V. Conclusion

From the results presented in Chapter IV several conclusions can be drawn concerning the validity of the various models assumed.

Under the conditions assumed in Chapter III the temperature model adequately predicts breakdown phenomena for incident laser fluxes above $5 \times 10^9 W/cm^2$. At these fluxes, the distribution function can be assumed to be maxwellian. In addition, at higher fluxes, the proportion of energy lost to ionizations is greater and the growth rate is not as strongly dependent on the shape of the distribution function. Below $5 \times 10^9 W/cm^2$ the temperature model is not reliable. The actual electron distribution is no longer adequately approximated by a maxwellian and the temperature model growth rates are too large. Finally, a two level atom can be assumed without significantly affecting the accuracy of the temperature model.

The results of Chapter IV indicate that the range over which the quantum kinetic and temperature model growth rates agree can be extended. A change in the excitation rate, ground state energy, and first excited state energy has a significant effect on the reliability of the temperature model. The low flux accuracy of the temperature model growth rates will improve as the excitation cross section decreases, the ground state energy decreases, and the first excited state energy increases. Therefore, the

temperature model will be most reliable when applied under the conditions of a low excitation cross section and a ratio of excitation energy to ionization energy near one.

Attempts to develop a simple model which would be valid at low fluxes proved unsucessful. The improved diffusion model possessed sufficient accuracy at high fluxes, but in the limit of low fluxes it was no better than the temperature model. The two-temperature model could not predict reasonable growth rates at any flux; therefore, it must be concluded that the assumption of a two-temperature distribution function is not valid.

Finally, it appears that the key to developing a simple breakdown model valid at low fluxes lies in a successful approximation of the electron distribution function. Therefore, any further investigation of breakdown at low fluxes should be directed toward the development of a distribution function which will adequately approximate the actual electron distribution function. One possible approach might be a modification of the temperature model distribution function to include an additional term which would depend on both the electron heating rate and the electron energy. At high fluxes this term would have little effect on the distribution function; however, at lower fluxes it would modify the distribution function sufficiently to permit an accurate prediction of the cascade growth rate.

Bibliography

1. Keldysh, L.V., "Ionization in the Field of a Strong Electromagnetic Wave", Soviet Physics JETP, 20, 1307-1314, (1965).

2. Zeldovich, Ya.B. and Raizer, Yu.P., "Cascade Ionization of a Gas by a Light Pulse", Soviet Physics JETP, 20, 772-779, (1965).

3. Raizer, Yu.P., "Breakdown and Heating of Gases Under the Influence of a Laser Beam", Soviet Physics Uspeckhi, 8, 650-672, (1966).

4. Brown, S.C., Introduction to Electrical Discharges in Gases, John Wiley & Sons, Inc., 1966.

5. Zeldovich, Ya.B. and Raizer, Yu.P., Physics of Shock Waves and High-Temperature Hydrodynamic Phenomena, Academic Press, 1966.

6. Phelps, A.V., "Theory of Growth of Ionization During Laser Breakdown", Physics of Quantum Electronics, 538-547, McGraw-Hill Book Co., 1966.

7. Brown, S.C., Basic Data of Plasma Physics, John Wiley & Sons, Inc., 1959.

8. Nielsen, P.E. and Canavan, G.H., "Electron Cascade Theory in Laser-Induced Breakdown of Preionized Gases", J. Appl. Phys., 44, 4224-4225, (1973).

9. Vyskrebentsev, A.I. and Raizer, Yu.P., "A Simple Theory of Breakdown of Monatomic Nonlight Gases in Fields of Any Frequency From Low to Optical", Soviet JAM and TP, 14, 32-38, (1973).

10. Allen, C.W., Astrophysical Quantities, The Althone Press, 1955.

11. Nielsen, P.E., "Notes on Gas Breakdown", unpublished.

12. Gear, C.W.,"The Automatic Integration of Ordinary Differential Equations", CACM, 14, 176-179, (1971).

13. Gear, C.W., "Difsub for Solution of Ordinary Differential Equations", CACM, 14, 185-190, (1971).

14. Handbook of Mathematical Functions, edited by M. Abramowitz and I.A. Stegun, Dover Publications, Inc., 1965.

15. Ostrowski, A.M., Solutions of Equations and Systems of Equations, Academic Press, 1966.

Appendix A

Cross Sections

A classical approach can be used to determine an analytic formula for the ionization cross section(Ref 5:392). If an electron of energy ϵ passes near another electron, the differential cross section for energy transfer to the target electron in a range $\Delta\epsilon$ to $\Delta\epsilon + d(\Delta\epsilon)$ is given by

$$d\sigma = \frac{\pi e^4}{(4\pi\epsilon_o)^2\epsilon} \frac{d(\Delta\epsilon)}{(\Delta\epsilon)^2} \tag{64}$$

Now, integrating this expression from I to ϵ yields the ionization cross section

$$\sigma(\epsilon) = \frac{\pi e^4}{(4\pi\epsilon_o)^2\epsilon} \frac{1}{I} - \frac{1}{\epsilon} \tag{65}$$

where I, the ionization energy, is the minimum energy that can be transferred. Thus, the cross section for ionization from the jth level can be written as

$$\sigma_j^I(\epsilon) = \frac{\pi e^4}{(4\pi\epsilon_o)^2 I_j} \frac{\epsilon - I_j}{\epsilon^2} \qquad \epsilon \geq I_j \tag{66}$$

where I_j represents the ionization energy of the jth level and ionization is assumed to occur each time an energy greater than I_j is transferred to an atom.

A simplified expression for the excitation cross

section is given by(Ref 10:40)

$$\sigma_{ij}^{x}(\epsilon) = \frac{\pi e^4}{(4\pi\epsilon_o)^2 x_{ij}} \frac{(\epsilon - x_{ij})}{\epsilon^2} 3f_{ij} \quad \begin{matrix} \epsilon \geq x \\ j>i \end{matrix} \tag{67}$$

where ϵ represents the energy of the free electron, $x_{ij} = I_i - I_j$ is the excitation energy between levels i and j, and f_{ij} is the oscillator strength for absorption given by(Ref 5:296)

$$f_{ij} = \frac{32}{3\pi\sqrt{3}} \frac{1}{n_i^5} \frac{1}{n_j^3} \frac{1}{(1/n_i^2 - 1/n_j^2)^3} \tag{68}$$

The value of the momentum transfer cross section, σ_m, for collisions between atoms and electrons, taken from Brown(Ref 7:5), was assumed to be constant over the electron energies of interest

$$\sigma_m = 7.1 \times 10^{-16} \text{ cm}^2 \tag{69}$$

Appendix B

Rates

The rate for the occurrence of ionization or excitation will depend on the cross section for the interaction and the relative velocity between the particles involved. Since the velocity of the electrons will be much greater than that of the atom, the velocity of the atom can be neglected so that the rate becomes

$$R(\epsilon) = \sqrt{\frac{2\epsilon}{m_e}}\,\sigma(\epsilon) \tag{33}$$

where ϵ is the energy of the electron and m_e its mass.

If the cross section for ionization is substituted into Eq (33) the rates of ionization used in the quantum kinetic model are obtained

$$R_j^I(\epsilon) = \sqrt{\frac{2}{m_e}}\,\frac{\pi e^4}{(4\pi\epsilon_o)^2 I_j}\,\epsilon^{-3/2}(\epsilon - I_j) \tag{34}$$

To obtain the ionization rate, $R^I(T)$, used in the temperature model, Eq (34) must be averaged over a maxwellian energy distribution

$$R_j^I(T) = \frac{2}{\sqrt{\pi}}\,\frac{1}{T^{3/2}}\int_I^\infty \epsilon^{1/2} R_j^I(\epsilon) e^{-\epsilon/T}\,d\epsilon \tag{70}$$

which upon integration becomes

$$R_j^I(T) = \frac{2^{3/2}\sqrt{\pi}e^4}{\sqrt{m_e}(4\pi\epsilon_o)^2 I_j} \frac{1}{T^{1/2}} \left[e^{-I_j/T} + E_i(-I_j/T)\right] \qquad (36)$$

where $E_i(-I_j/T)$ is given by Eq (37). Similarly, the rates of excitation for the quantum kinetic model can be given by

$$R_{ij}^x(\epsilon) = \sqrt{\frac{2}{m_e}} \frac{\pi e^4}{(4\pi\epsilon_o)^2 x_{ij}} \epsilon^{-3/2}(\epsilon - x_{ij}) 3f_{ij} \qquad (35)$$

and the corresponding temperature model rate is

$$R_{ij}^x(T) = \frac{2^{3/2}\sqrt{\pi}e^4 3f_{ij}}{\sqrt{m_e}(4\pi\epsilon_o)^2 x_{ij}} \frac{1}{T^{1/2}} \left[e^{-x_{ij}/T} + \frac{x_{ij}}{T} E_i(-x_{ij}/T)\right] \qquad (38)$$

Table X gives compact numerical formulas for the various rates.

Table X

Rates of Ionization and Excitation

	R(ε)	R(T)
R_1^I	$2.76\times10^{-7}\epsilon^{-3/2}(\epsilon - 14)$	$2.45\times10^{-7}T^{-1/2}\ e^{-14/T} + 14T^{-1}E_i(\frac{-14}{T})$
R_2^I	$1.10\times10^{-6}\epsilon^{-3/2}(\epsilon - 3.5)$	$9.78\times10^{-7}T^{-1/2}\ e^{-3.5/T} + 3.5T^{-1}E_i(\frac{-3.5}{T})$
R_3^I	$2.48\times10^{-6}\epsilon^{-3/2}(\epsilon - 1.56)$	$2.19\times10^{-7}T^{-1/2}\ e^{-1.56/T} + 1.56T^{-1}E_i(\frac{-1.56}{T})$
R_{12}^x	$6.41\times10^{-7}\epsilon^{-3/2}(\epsilon - 10.5)$	$5.68\times10^{-7}T^{-1/2}\ e^{-10.5/T} + 10.5T^{-1}E_i(\frac{-10.5}{T})$
R_{13}^x	$9.63\times10^{-8}\epsilon^{-3/2}(\epsilon - 12.44)$	$8.53\times10^{-8}T^{-1/2}\ e^{-12.44/T} + 12.44T^{-1}E_i(\frac{-12.44}{T})$
R_{23}^x	$5.06\times10^{-6}\epsilon^{-3/2}(\epsilon - 1.94)$	$4.48\times10^{-6}T^{-1/2}\ e^{-1.56/T} + 1.56T^{-1}E_i(\frac{-1.56}{T})$

Appendix C

Derivation of the Temperature Model

Using a method similar to that of Ref 11 the temperature model can be derived from the quantum kinetic equation for the time rate of change of the electron distribution function, Eq (23), where $f(\epsilon)$ is assumed maxwellian. For small $\hbar\omega/\epsilon$, the bremsstrahlung absorption and emission terms can be expanded in a Taylor series and in the limit as $\hbar\omega/\epsilon \rightarrow 0$ Eq (23) becomes(Ref 2:774,776)

$$\frac{\partial f(\epsilon)}{\partial t} = \frac{\dot{\epsilon}}{n_e}\frac{\partial f(\epsilon)}{\partial \epsilon} - \sum_{i,j} n_i R_{ij}^X(\epsilon) f(\epsilon)$$

$$+ \sum_{i,j} n_i R_{ij}^X(\epsilon + x_{ij}) f(\epsilon + x_{ij}) - \sum_j n_j R_j^I(\epsilon) f(\epsilon)$$

$$+ \sum_j n_j R_j^I(\epsilon + I_j) f(\epsilon + I_j)$$

$$+ \delta(\epsilon) \sum_j n_j \int_0^\infty R_j^I(\epsilon) f(\epsilon) d\epsilon \qquad (71)$$

where $\dot{\epsilon}$ is the classical microwave heating rate given by Eq (9).

An equation for the time rate of charge of n_e can be obtained by taking the zeroth energy moment of Eq (71). Integrating the equation over all energy yields

$$\frac{dn_e}{dt} = n_e \sum_j n_j \langle R_j^I \rangle \qquad (43)$$

To obtain an equation for the time rate of change of $\langle\epsilon\rangle$, the average energy, the first energy moment of Eq (71) is taken. Multiplying the equation by ϵ and integrating over all energy yields

$$\frac{d\langle\epsilon\rangle}{dt} = \frac{\dot{\epsilon}}{n_e} - \sum_j n_j I_j \langle R_j^I \rangle$$

$$- \sum_{i,j} n_i x_{ij} \langle R_{ij}^x \rangle - \frac{\langle\epsilon\rangle}{n_e} \frac{dn_e}{dt} \tag{44}$$

where the non-zero terms of the integration are

$$\int_0^\infty \epsilon \frac{\partial f(\epsilon)}{\partial t} d\epsilon = n_e \frac{d\langle\epsilon\rangle}{dt} + \langle\epsilon\rangle \frac{dn_e}{dt} \tag{72}$$

$$\int_0^\infty \epsilon \sum_{i,j} n_i R_{ij}^x(\epsilon) f(\epsilon) d\epsilon - \int_0^\infty \epsilon \sum_{i,j} n_i R_{ij}^x(\epsilon$$

$$+ x_{ij}) f(\epsilon + x_{ij}) d\epsilon = n_e \sum_{i,j} n_i x_{ij} \langle R_{ij}^x \rangle \tag{73}$$

$$\int_0^\infty \epsilon \sum_j n_j R_j^I(\epsilon) f(\epsilon) d\epsilon - \int_0^\infty \epsilon \sum_j n_j R_j^I(\epsilon$$

$$+ I_j) f(\epsilon + I_j) d\epsilon = n_e \sum_j n_j I_j \langle R_j^I \rangle \tag{74}$$

$\langle R \rangle$ being the energy average of the ionization or excitation rate, and $\langle\epsilon\rangle = (3/2)T$ for a maxwellian, where T is defined to be the electron temperature.

The equations for the time rate of change of the n_i can be written as

$$\frac{dn_i}{dt} = - n_e n_i R_i^I - \sum_{j>i} \langle R_{ij}^x \rangle n_i n_e + \sum_{j<i} \langle R_{ij}^x \rangle n_j n_e \quad (75)$$

These three equations together with Eqs (43)-(44) form the set of equations which comprise the temperature model.

Appendix D

Numerical Solution of the Quantum Kinetic Model

The equations to be solved are the quantum kinetic equation (23), and the equations representing the changes in the population of the three atomic levels, Eqs (39)-(41). The method of solution employed is similar to the one used in Ref 8.

Eq (23), as written, cannot be readily solved, since the form of the distribution function is unknown. However, if the energy axis is divided into K discrete bins of width $\hbar\omega$ Eq (23) is transformed into K equations of the form

$$\frac{df_m}{dt} = n_a F\left[a_{m-1}f_{m-1} - (a_m + b_m)f_m + b_{m+1}f_{m+1}\right]$$

$$- \sum_j n_j R^I_{jm} f_m + \sum_j n_j R^I_{j,m+I_j} f_{m+I_j} - \sum_{i,j>i} n_i R^x_{ijm} f_m$$

$$+ \sum_{i,j>i} n_i R^x_{ij,m+x_{ij}} f_{m+x_{ij}} + \delta_{m1} \sum_{j,k} n_j R^I_{j,k} f_k \qquad (76)$$

where f_m represents the value of the electron distribution function at energy $\epsilon_m = (m - 1/2)h\omega$, the midpoint of the mth bin. R_m, a_m, and b_m are the corresponding values for the various rates at energy ϵ_m, while I_j and x_{ij} are integers which represent the mumber of bins which correspond to the various ionization and excitation energies. Eq (76) together with Eqs (39)-(41) can now be solved.

The initial conditions are established by specifying the temperature of the gas, the photon flux, the number of ground state atoms, the number of electrons present as a result of non-equilibrium effects(i.e. pre-ionization), the number of bins, and the bin width. The populations of the second and third atomic levels are calculated assuming a Boltzmann distribution

$$n_i = n_1 \, e^{-x_{1i}/T_o} \tag{77}$$

where T_o is the gas temperature and the degeneracy of each level is assumed to be 1. The total free electron population is determined by adding the equilibrium electron population, as determined by the Saha equation

$$n_e = (2n_a)^{1/2}\left[\frac{2\pi m_e T_o}{h^2}\right]^{3/4} e^{-I/2T_o} \tag{78}$$

to the population resulting from non-equilibrium effects. The electron population of each bin is then calculated by integrating a Maxwell-Boltzmann distribution function over the width of the bin

$$f_m = \frac{2}{\sqrt{\pi}} \int_{\epsilon_m+(h\omega)/2}^{\epsilon_m-(h\omega)/2} \frac{\epsilon^{1/2}}{T^{3/2}} e^{-\epsilon/T} \, d\epsilon \tag{79}$$

Each bin is assumed to have a minimum initial population of one electron.

The rates for excitation and ionization are calculated

for all bins which possess an energy, ϵ_m, greater than the threshold energy of the corresponding rate. They are calculated by substituting the value of ϵ_m into the appropriate rates found in table X. The coefficients of bremsstrahlung absorption are calculated for each bin using

$$a_m = \frac{2e^2}{3m_e c \epsilon_o \omega^2}\left[\frac{2(\epsilon_m + \hbar\omega)}{m_e}\right]^{1/2} \frac{(\epsilon_m + \hbar\omega/2)}{\hbar\omega}\sigma_m \qquad (80)$$

where σ_m is a constant given by Eq (69). The coefficient for bremsstrahlung emission is calculated for each bin by microreversibility

$$b_m = a_{m-1}\left[\frac{\epsilon_m}{\epsilon_m + \hbar\omega}\right]^{1/2} \qquad (81)$$

The emission and absorption rates are then obtained by multiplying the emission and absorption coefficients by the scaled photon flux. The scaling of the incident flux allows the choice of a convenient bin width, $\hbar\omega$, which does not correspond to the actual photon energy, $\hbar\omega_1$, of the incident radiation. The relationship between the actual and scaled fluxes is given by

$$F = \frac{S}{(\hbar\omega_1)^2}\hbar\omega \qquad (82)$$

where S is in W/cm^2 and F is in $\#/(cm^2\text{-sec})$. The scaling of Eq (82) yields a correct net absorption rate for $\hbar\omega/\epsilon$ small. To show this, the net absorption rate is expanded

in a Taylor series which in the limit as $\hbar\omega/\epsilon \rightarrow 0$ yields (Ref 2:776)

$$\dot{\epsilon} \propto \frac{S}{\omega^2} \tag{83}$$

where $\dot{\epsilon}$ is the net bremsstrahlung absorption rate and S is the laser flux in W/cm^2.

With the initial conditions established Eqs (39)-(41) and (76) are solved in time using an algorithm, developed by Gear(Ref 12,13), for the solution of stiff systems of first order ordinary differential equations. This scheme employs multistep predictor-corrector methods of up to sixth order. The error for each step is defined by

$$\epsilon = \left\{ \sum_i \left[\frac{(\Delta t)^{k+1} x_i^{(k+1)}}{(k+1) x_i^{max}} \right]^2 \right\}^{1/2} \tag{84}$$

where the x_i's are the solutions to the set of equations, k is the order, Δt is the time step, $x_i^{(k+1)}$ is the (k+1) derivative of x_i, and x_i^{max} is the maximum value of the x_i encountered. A step is accepted and the time advanced when the error is less than .01 . The solution of the equations is terminated once a specified value of the free electron density is achieved.

Appendix E

Numerical Solution of the Temperature Model

The equations to be solved are the equations for the change in population of the three atomic levels, Eqs (39)-(41), and the equations for the zeroth and first energy moments of the Boltzmann equation, Eqs (43) and (44). Eq (44) becomes, upon setting $\langle\epsilon\rangle = (3/2)T$,

$$\frac{dT}{dt} = \frac{2}{3}\left[\frac{\dot{\varepsilon}}{n_e} - \sum_j n_j I_j R_j^I(T) - \sum_{i,j>i} n_i x_{ij} R_{ij}^x(T)\right] - \frac{T}{n_e}\frac{dn_e}{dt} \qquad (85)$$

The initial conditions are established in a manner quite similar to that used in the quantum kinetic solution. The gas temperature, laser flux, density of ground state atoms, and density of non-equilibrium electrons are specified. The populations of the remaining atomic levels are calculated using Eq (77). The total free electron density is determined by adding the result of Eq (78) to the non-equilibrium density. The heating rate is calculated using Eq (9). Finally, the rates as a function of temperature are calculated from

$$R^I(T) = \frac{C}{T^{3/2}} \int_I^\infty \frac{\epsilon - I}{\epsilon} e^{-\epsilon/T}\, d\epsilon \qquad (86)$$

which upon integration becomes

$$R^I(T) = (C/T^{3/2})[Te^{-I/T} + I\, E_i(-I/T)] \qquad (87)$$

where I now represents either the ionization or excitation energy, C is a constant, and $E_i(-I/T)$ is the integral defined in Eq (37) and is evaluated using algorithms found in the Handbook of Mathematical Functions(Ref 14:231).

The solution to the set of equations, (39)-(41), (43) and (85), is obtained by using a second order predictor-corrector method. The equations are all of the form

$$\dot{x}_i = f(x_i, x_j, \cdots x_s) \qquad (88)$$

The various $\dot{x}_i$'s are first computed utilizing Eqs (39)-(41) (43) and (85), and the initial conditions at t_o. A predicted value of x_i at $t = t_o + \Delta t$ is then computed

$$x_i^p = x_i + \dot{x}_i \Delta t \qquad (89)$$

The derivative $\dot{x}_i^p$ is computed and used to obtain a corrected value of x_i at t_1

$$x_i^c = x_i + \frac{\Delta t}{2}(\dot{x}_i + \dot{x}_i^p) \qquad (90)$$

The predicted and corrected values are compared and if the error as defined by

$$\epsilon = \sum_i \frac{|x_i^p - x_i^c|}{x_i} \qquad (91)$$

is less than .01, the solution is accepted, the time advanced from t_o to t_1, and a new iteration is begun with Δt doubled. If the error is greater than .01, the solution is rejected, Δt is reduced by a half, and the calculation repeated. This process is then continued until the solution at a particular time is obtained, or a specified value of any of the x_i is reached.

Appendix F

Derivation of the Second Energy Moment of the Boltzmann Equation

The solution of the two-temperature model requires the use of an additional equation. This equation can be obtained by taking the second energy moment of the Boltzmann equation, Eq (11). Multiplying Eq (11) by ϵ^2 and integrating over all energy yields an equation for the time rate of change of $<\epsilon^2>$

$$\frac{d<\epsilon^2>}{dt} = 2\frac{\dot{\epsilon}}{n_e}<\epsilon> + x^2 n_1 <R^x> + I^2 n_1 <R^I>$$

$$- 2xn_1<\epsilon R^x> - 2In_1<\epsilon R^I> - \frac{<\epsilon^2>}{n_e}\frac{dn_e}{dt} \qquad (59)$$

where the non-zero terms of the integration are

$$\int_0^\infty \epsilon^2 \frac{\partial f}{\partial t}\, d\epsilon = n_e \frac{d<\epsilon^2>}{dt} + <\epsilon^2>\frac{dn_e}{dt} \qquad (92)$$

$$\frac{\dot{\epsilon}}{n_e}\int_0^\infty \epsilon^2 \frac{\partial f}{\partial \epsilon}\, d\epsilon = -2\dot{\epsilon}<\epsilon> \qquad (93)$$

$$n_1 \int_0^\infty \epsilon^2 f(\epsilon + x)R^x(\epsilon + x)d\epsilon - n_1 \int_0^\infty \epsilon^2 f(\epsilon)R^x(\epsilon)d\epsilon =$$

$$x^2 n_1 n_e <R^x> - 2xn_1 n_e <\epsilon R^x> \qquad (94)$$

$$n_1 \int_0^\infty \epsilon^2 f(\epsilon + I) R^I(\epsilon + I) d\epsilon - n_1 \int_0^\infty \epsilon^2 f(\epsilon) R^I(\epsilon)\, d\epsilon =$$

$$I^2 n_1 n_e \langle R^I \rangle - 2I n_1 n_e \langle \epsilon R^I \rangle \qquad (95)$$

The < > describes the average of the enclosed quantity over the appropriate distribution function.

Appendix G

Numerical Solution of the Two-Temperature Model

The equations to be solved are the equations for the zeroth, first, and second energy moments of the Boltzmann equation, Eqs (13)-(14) and (59), subject to the conditions of Eqs (55)-(57). Assuming a rapid equilibration of $\langle\epsilon\rangle$ and $\langle\epsilon^2\rangle$ Eqs (14) and (59) upon substitution for dn_e/dt become

$$\frac{\dot{\epsilon}}{n_e} - xn_1\langle R^x\rangle - (I + \langle\epsilon\rangle)n_1\langle R^I\rangle = 0 \tag{58}$$

$$2\frac{\dot{\epsilon}}{n_e}\langle\epsilon\rangle + x^2 n_1\langle R^x\rangle + (I^2 - \langle\epsilon^2\rangle)n_1\langle R^I\rangle$$

$$-2xn_1\langle\epsilon R^x\rangle - 2In_1\langle\epsilon R^I\rangle = 0 \tag{60}$$

Before Eqs (58) and (60) can be solved, the averaged quantities in each equation must be evaluated using the two-temperature distribution function, Eq (55). The average value of the energy, $\langle\epsilon\rangle$, is given by

$$C_1 \int_0^x \epsilon^{3/2} e^{-\epsilon/T_1}\, d\epsilon + C_2 \int_x^\infty \epsilon^{3/2} e^{-\epsilon/T_2}\, d\epsilon =$$

$$C_1 T_1^{5/2}[\Gamma(5/2) - \Gamma(5/2, x/T_1)] + C_2 T_2^{5/2}\Gamma(5/2, x/T_2) \tag{96}$$

where the gamma function is defined by(Ref 14:255)

$$\Gamma(x) = \int_0^\infty t^{x-1}\, e^{-t}\, dt \tag{97}$$

and the incomplete gamma function is given by(Ref 14:260)

$$\Gamma(a,x) = \int_x^\infty t^{a-1}\, e^{-t}\, dt \tag{98}$$

The value of $<\epsilon^2>$ is given by

$$C_1 \int_0^x \epsilon^{5/2} e^{-\epsilon/T_1}\, d\epsilon + C_2 \int_x^\infty \epsilon^{5/2} e^{-\epsilon/T_2}\, d\epsilon =$$

$$C_1 T_1^{7/2}[\Gamma(7/2) - \Gamma(7/2,x/T_1)] + C_2 T_2^{7/2}\Gamma(7/2,x/T_2) \tag{99}$$

Using Eqs (36) and (38) the average values of the ionization and excitation rate can be written as

$$<R^I> = (2.76\text{x}10^{-7})C_2[T_2 e^{-I/T_2} + I\, E_i(-I/T_2)] \tag{100}$$

$$<R^x> = (6.41\text{x}10^{-7})C_2[T_2 e^{-x/T_2} + x\, E_i(-x/T_2)] \tag{101}$$

where E_i is defined by Eq (37). Finally, the averages $<\epsilon R^I>$ and $<\epsilon R^x>$ upon integration become

$$<\epsilon R^I> = (2.76\text{x}10^{-7})C_2 T_2^2\, e^{-I/T_2} \tag{102}$$

$$<\epsilon R^x> = (6.41\text{x}10^{-7})C_2 T_2^2\, e^{-x/T_2} \tag{103}$$

The constants C_1 and C_2 must now be expressed in terms of T_1 and T_2. Solving Eq (56) for C_1 yields

$$C_1 = C_2 \, e^{-x/T_2} \, e^{x/T_1} \tag{104}$$

Integrating Eq (57) and substituting for C_1 using Eq (104) yields

$$C_2 = \left\{ T_1^{3/2} \, e^{-x/T_2} \, e^{x/T_1} [\Gamma(3/2) \right.$$

$$\left. - \Gamma(3/2, x/T_1)] + T_2^{3/2} \Gamma(3/2, x/T_2) \right\}^{-1} \tag{105}$$

Eqs (58) and (60) can now be solved for T_1 and T_2 using an iterative procedure(Ref 15:239). Eqs (58) and (60) are first written as

$$F(T_1,T_2) = \frac{\dot{\epsilon}}{n_e} - x n_1 \langle R^x \rangle - (I + \langle \epsilon \rangle) n_1 \langle R^I \rangle \tag{106}$$

$$G(T_1,T_2) = 2\frac{\dot{\epsilon}}{n_e} \langle \epsilon \rangle + x^2 n_1 \langle R^x \rangle + (I^2 - \langle \epsilon^2 \rangle) n_1 \langle R^I \rangle$$

$$-2x n_1 \langle \epsilon R^x \rangle - 2I n_1 \langle \epsilon R^I \rangle \tag{107}$$

The functions $F(T_1,T_2)$ and $G(T_1,T_2)$ are then evaluated at three points $(T_1,T_2)_a$, $(T_1,T_2)_b$, and $(T_1,T_2)_c$ which are estimates of the actual solution (T_1,T_2), to Eqs (58) and (60). An improved estimate, $(T_1,T_2)_d$, is obtained using

$$T_{id} = \frac{\det \begin{bmatrix} T_{ia} & T_{ib} & T_{ic} \\ F_a & F_b & F_c \\ G_a & G_b & G_c \end{bmatrix}}{\det \begin{bmatrix} 1 & 1 & 1 \\ F_a & F_b & F_c \\ G_a & G_b & G_c \end{bmatrix}} \qquad i = 1,2 \qquad (108)$$

The improved estimate is used to replace one of the original estimates and the iteration is repeated. This procedure is continued until successive estimates of (T_1, T_2) agree to within .01 eV. The constant C_2 is then computed using Eq (105) and the electron growth rate obtained using

$$R = (2.76 \times 10^{-7}) n_1 C_2 [T_2 e^{-I/T_2} + I\, E_i(-I/T_2)] \qquad (109)$$

where n_1 is the ground state population.

VITA

David A. Kloc was born on 23 January 1950 in Buffalo, New York. He graduated from St. Francis High School in Athol Springs, New York in 1967 and attended Rensselaer Polytechnic Institute from which he received the degree of Bachelor of Science in physics in June 1971. Upon graduation he was commissioned as a Second Lieutenant in the USAF. Upon entering active duty in August 1971, he attended Communications Systems Officers' School at Keesler AFB, Mississippi graduating in February 1972. He then served as a communications systems officer and chief of maintenance with the 1928th Communications Group, MacDill AFB, Florida until entering the School of Engineering, Air Force Institute of Technology, in June 1975.

Permanent address: 97 South Drive
Lackawanna, New York 14218

UNCLASSIFIED

SECURITY CLASSIFICATION OF THIS PAGE (When Data Entered)

REPORT DOCUMENTATION PAGE		READ INSTRUCTIONS BEFORE COMPLETING FORM
1. REPORT NUMBER GEP/PH/76-7	2. GOVT ACCESSION NO.	3. RECIPIENT'S CATALOG NUMBER
4. TITLE (and Subtitle) GAS BREAKDOWN CALCULATIONS: A COMPARATIVE STUDY		5. TYPE OF REPORT & PERIOD COVERED MS Thesis 6. PERFORMING ORG. REPORT NUMBER,
7. AUTHOR(s) David A. Kloc Capt USAF		8. CONTRACT OR GRANT NUMBER(s)
9. PERFORMING ORGANIZATION NAME AND ADDRESS Air Force Institute of Technology (AFIT-EN) Wright-Patterson AFB, Ohio 45433		10. PROGRAM ELEMENT, PROJECT, TASK AREA & WORK UNIT NUMBERS
11. CONTROLLING OFFICE NAME AND ADDRESS Air Force Weapons Laboratory (AFWL/DYT) Kirtland AFB, New Mexico 87117		12. REPORT DATE December 1976 13. NUMBER OF PAGES 91
14. MONITORING AGENCY NAME & ADDRESS(if different from Controlling Office)		15. SECURITY CLASS. (of this report) Unclassified 15a. DECLASSIFICATION/DOWNGRADING SCHEDULE

16. DISTRIBUTION STATEMENT (of this Report)

Approved for public release; distribution unlimited

17. DISTRIBUTION STATEMENT (of the abstract entered in Block 20, if different from Report)

18. SUPPLEMENTARY NOTES

Approved for public release; IAW AFR 190-17

JERRAL F. GUESS, Captain, USAF
Director of Information

19. KEY WORDS (Continue on reverse side if necessary and identify by block number)

Laser-induced Gas Breakdown
Quantum Kinetic Model
Temperature Model

20. ABSTRACT (Continue on reverse side if necessary and identify by block number)

An attempt is made to develop a simple yet accurate gas breakdown model which can be easily coupled to the hydrodynamic equations governing fluid flow in laser-target interactions. The accuracy of three relatively simple models is investigated. Each is compared with the more accurate and complex quantum kinetic model. A gas consisting of a single monatomic species is assumed and attention is restricted to the early portion of the electron cascade. A temperature model is found to agree reasonably well with the quantum kinetic model at values→

next page

DD FORM 1 JAN 73 1473 EDITION OF 1 NOV 65 IS OBSOLETE

SECURITY CLASSIFICATION OF THIS PAGE (When Data Entered)

cont →

of incident laser flux greater than 5×10^9 W/cm^2. A diffusion model is found to yield similar results. A two-temperature model, which is derived in an attempt to extend the range of the temperature model to lower values of incident flux, is found to be invalid.